US Army Corps
of Engineers
Construction Engineering
Research Laboratory

USACERL Technical Report N-90/09
May 1990

(2)

Methods for Detecting Low-Frequency Signals in the Presence of Strong Winds

by
Paul D. Schomer
Richard Raspet
Mark Wagner
Douglas Walker
Daniel Marshall
John Brunner

This report looks at two methods to better separate bl. .t noise from wind induced noise in unattended monitoring situations. One method is to use a windscreen, a device which prevents wind and wind induced pressures from reaching the microphone diaphragm while allowing the unimpeded passage of true acoustical pressures to the microphone. The second method is to make the microphone-black box system "smarter" so that it can separate wind induced noise from true blast noise.

The results show both methods can do a good job of reducing wind induced noise. For blast noise, where the C-weighted sound is relevant, a special, two-layer wind screen can reduce the C-weighted sound level by almost 30 dB as compared with a bare microphone. Taking the integrated cross product of two vertically spaced microphones (about 60 cm spacing) reduces the C-weighted noise as compared with a bare microphone by about 22 dB. The two methods can be combined, but only when the wind induced noise level is very high and the C-weighted background noise ambient is very low. Otherwise, the two methods together are too good; the maximum useful reduction is the difference between the wind noise level and the background acoustical ambient

The contents of this report are not to be used for advertising, publication, or promotional purposes. Citation of trade names does not constitute an official indorsement or approval of the use of such commercial products. The findings of this report are not to be construed as an official Department of the Army position, unless so designated by other authorized documents.

DESTROY THIS REPORT WHEN IT IS NO LONGER NEEDED

DO NOT RETURN IT TO THE ORIGINATOR

REPORT DOCUMENTATION PAGE

Form Approved
OMB No. 0704-0188

1. AGENCY USE ONLY (Leave blank)	2. REPORT DATE	3. REPORT TYPE AND DATES COVERED
	May 1990	Final

4. TITLE AND SUBTITLE
Methods for Detecting Low-Frequency Signals in the Presence of Strong Winds

5. FUNDING NUMBERS
PE 4A162720
PR A896
WU UJ9

6. AUTHOR(S)
Paul D. Schomer, Richard Raspet, Mark Wagner, Douglas Walker, Daniel Marshall, and John Brunner

7. PERFORMING ORGANIZATION NAME(S) AND ADDRESS(ES)
U.S. Army Construction Engineering Research Laboratory
P.O. Box 4005
Champaign, IL 61824-4005

8. PERFORMING ORGANIZATION REPORT NUMBER
USACERL TR N-90/09

9. SPONSORING/MONITORING AGENCY NAME(S) AND ADDRESS(ES)
U.S. Army Engineering and Housing Support Center
Fort Belvoir, VA 22060

Office of the Chief of Engr
Army Environmental Office
ATTN: ENVR-ER
Room 1E677, Pentagon
Washington, DC 20310-2600

10. SPONSORING/MONITORING AGENCY REPORT NUMBER

11. SUPPLEMENTARY NOTES
Copies are available from the National Technical Information Service, 5285 Port Royal Road, Springfield, VA 22161.

12a. DISTRIBUTION/AVAILABILITY STATEMENT
Approved for public release; distribution is unlimited.

12b. DISTRIBUTION CODE

13. ABSTRACT *(Maximum 200 words)*

This report looks at two methods to better separate blast noise from wind induced noise in unattended monitoring situations. One method is to use a windscreen, a device which prevents wind and wind induced pressures from reaching the microphone diaphragm while allowing the unimpeded passage of true acoustical pressures to the microphone. The second method is to make the microphone-black box system "smarter" so that it can separate wind induced noise from true blast noise.

The results show both methods can do a good job of reducing wind induced noise. For blast noise, where the C-weighted sound is relevant, a special, two-layer wind screen can reduce the C-weighted sound level by almost 30 dB as compared with a bare microphone. Taking the integrated cross product of two vertically spaced microphones (about 60 cm spacing) reduces the C-weighted noise as compared with a bare microphone by about 22 dB. The two methods can be combined, but only when the wind induced noise level is very high and the C-weighted background noise ambient is very low. Otherwise, the two methods together are too good; the maximum useful reduction is the difference between the wind noise level and the background acoustical ambient.

14. SUBJECT TERMS	15. NUMBER OF PAGES
blast noise wind noise monitoring	113
	16. PRICE CODE

17. SECURITY CLASSIFICATION OF REPORT	18. SECURITY CLASSIFICATION OF THIS PAGE	19. SECURITY CLASSIFICATION OF ABSTRACT	20. LIMITATION OF ABSTRACT
Unclassified	Unclassified	Unclassified	SAR

FOREWORD

This work was funded by the U.S. Army Engineering and Housing Support Center (USAEHSC) under Project 4A162720A896, "Environmental Quality Technology"; Work Unit UJ9, "Technology to Reduce Noise Impacts of Training Activities." The Technical Monitor was LTC H. Graven, ENVR-EP.

Mark Wagner, Douglas Walker, Daniel Marshall, and John Brunner have completed Masters Theses in Electrical Engineering at the University of Illinois at Urbana-Champaign. Large portions of the latter three theses form the bulk of this report. Dr. Paul D. Schomer and Richard Raspet, Environmental Division (EN) at USACERL, were advisors for this work, and Dr. Schomer acted as general editor for the report. Dr. R. K. Jain is Chief, USACERL-EN.

LTC E.J. Grabert, Jr. is Commander of USACERL, and Dr. L.R. Shaffer is Director.

CONTENTS

FIGURES

TABLES

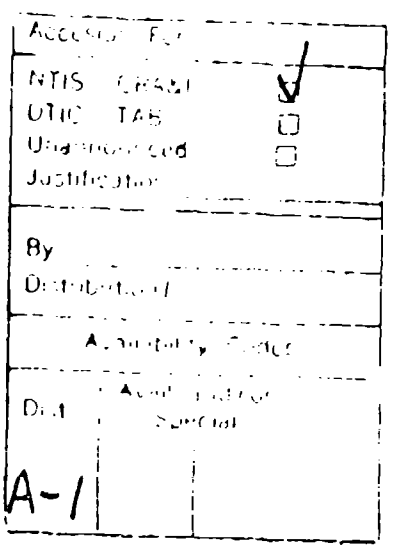

METHODS FOR DETECTING LOW-FREQUENCY SIGNALS IN THE PRESENCE OF STRONG WINDS

1 INTRODUCTION

Background

Environmental noise is a major challenge of modern technological society. Manufacturing, motor vehicles and aircraft are major noise sources in urban areas. Around Army installations, the low frequency noise generated by helicopters and large weapons becomes a major environmental noise problem. Naturally, quantification is one facet of a comprehensive program designed to manage and mitigate a major noise problem.

Typically, the magnitude of a noise problem is quantified in one of two ways: (1) computer simulations are used to predict contours of equal average sound energy, or (2) direct measurement is used to quantify the problem. Sometimes, such as with airports, monitoring systems are used to verify and/or adjust computer simulations. In any case, when direct measurement or monitoring is employed, the goal is to measure just the source of noise in question: the airport or the single airplane, the factory, the downtown heliport, or the noise from big guns on an Army base.

When using an unattended monitoring system, or "black box," the challenge is to isolate the source of noise of interest, so that extraneous

noise is not measured. Near Army installations wind is the culprit. Here, the goal may be to measure just the large-weapon blast noise, but the wind-induced noise looks just like blast noise to the monitor.

Outside, wind is ubiquitous. Even on the calmest days in seemingly well sheltered areas, air flow velocities seldom drop below 0.5 m/sec; on windy days they can often exceed 10 m/sec. The wind is *not* an acoustic signal. Some small fraction of its energy may be radiated as an acoustic pressure wave, but a large percentage of it is simply a mean flow of particles whose speed is much less than the speed of sound. In essence, this air flow can affect the diaphragm or other pressure sensor of a microphone in exactly the same way a real acoustic signal does. There is a mechanical movement which yields an electrical response which is virtually indistinguishable from that of a true acoustic signal.

The energy in blast noise from a large weapon peaks in about the 15 to 40 Hz range, and there is little energy above about 200 Hz [Ref. 1]. As will be shown, wind noise is also concentrated at almost the same low frequencies, and it can very effectively mask blast noise. So, if one tries to measure only blast noise but must do this in the presence of wind, there are three possible outcomes: (1) a blast occurred and is measured, (2) a blast occurred but the "black box" thought it was wind and did not measure it, or (3) a wind signal occurred but the "black box" thought it was a blast

and measured it. Even for case (1) where there is a blast and the "black box" thinks it is a blast and measures it, the signal is corrupted; the wind signal adds to the blast signal.

Purpose

The purpose of this research is to develop acoustical and electronic hardware which can minimize wind noise while allowing the undistorted passage of blast signals to the microphone and analysis instrumentation.

Approach

This report looks at two methods to better separate blast noise from wind induced noise in unattended monitoring situations. One method is windscreens which prevent wind and wind induced pressures from reaching the microphone diaphragm while allowing the unimpeded passage of true acoustical pressures to the microphone. The second method is to make the microphone/black box system "smarter" so it can separate wind induced noise from true blast noise.

Mode of Technology Transfer

The methods developed in this study will be made available to the private sector so that retrofit and new windscreens on the Army's unattended blast noise measurement and monitoring systems can better detect and measure gun noise.

2 WINDSCREENS

A microphone "windscreen" is defined as a device which reduces turbulent airflow incident upon a microphone. This turbulence is of two kinds. The first is *intrinsic* turbulence, that occurring naturally in atmospheric airflows. The second is *induced* turbulence, which results from the insertion of a microphone or a windscreen into the flow. The turbulence causes pressure fluctuations on the diaphragm of the microphone which are not due to real acoustic signals; that is, pressure fluctuations which (except for a small percentage) are not independent of the mean flow of the medium. In spite of the physical differences between this turbulence and acoustic waves, the effect it has on a microphone is indistinguishable from that of a real acoustic wave. In particular, the response of a microphone due to a small, localized eddy may be very similar to the response due to a blast wave. This is illustrated by two actual microphone recordings shown in Figure 1: one with an unscreened and one with a screened microphone. The blast signal cannot be detected in the unscreened recording because the wind-induced signal is as large or larger than the blast signal. For these reasons, the phenomenon of apparent sound caused by turbulent airflow across a microphone has been called "pseudosound" or wind noise. The task of a windscreen is to reduce wind noise by minimizing turbulent airflow at

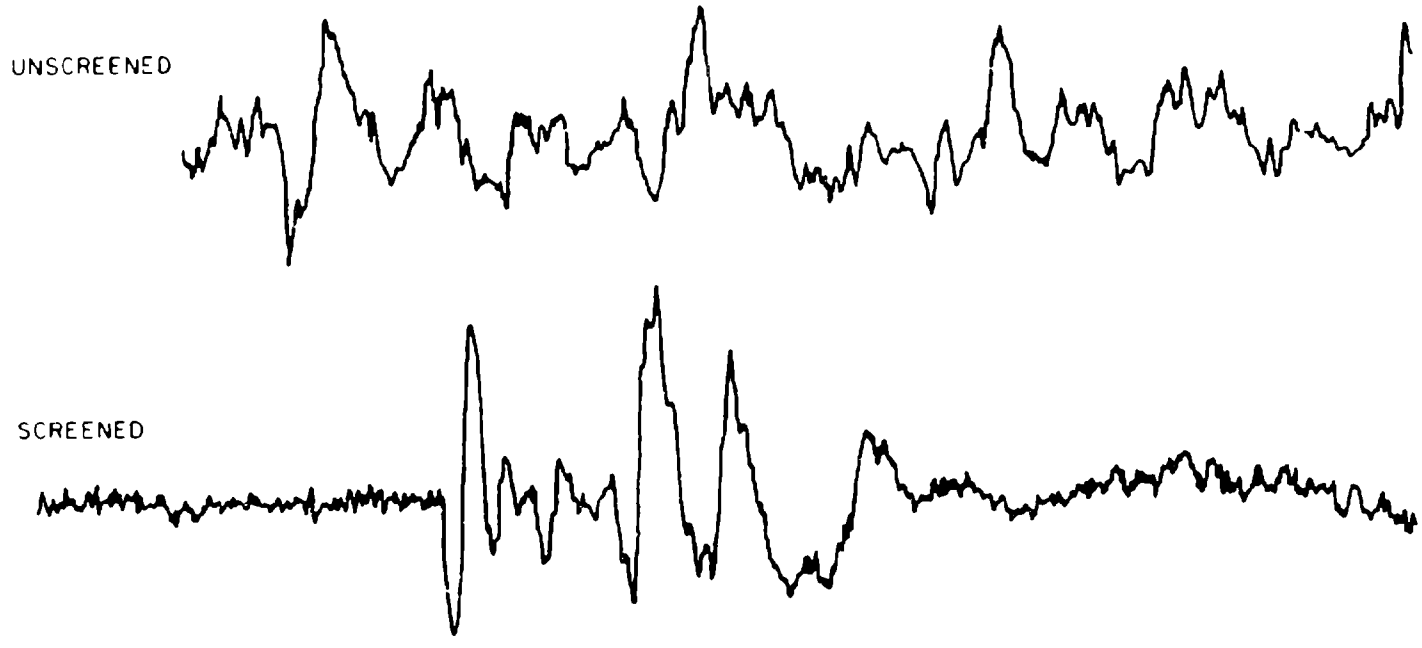

Figure 1. Actual microphone recordings.

the microphone diaphragm. It should not, of course, block the acoustic wave. Realistically, though, any windscreen is bound to allow *some* turbulent airflow and to produce *some* attenuation of the acoustic wave.

Historically, the problem of windscreening has been approached from several directions. For wind incident from one given direction, it has been shown that solid, aerodynamic cones and slit tubes can block the wind effectively without serious effects on the acoustic signal [Ref. 2-6]. Real field conditions, however, require effective screening in all directions, for which a solid windscreen is not feasible. Therefore, most field windscreens surround the microphone with a semipermeable "membrane" which is intended to decrease the airflow and, therefore, the turbulence across the microphone diaphragm. In so doing, of course, the windscreen introduces its own turbulence, but this turbulence is generated at roughly the windscreen radius away from the microphone and thus has less effect.

Attempts to mathematically quantify the effects of windscreens have met with only limited success. In 1938, Pnelps developed an expression for the pressure around a sphere subject to an incompressable, nonturbulent flow [Ref. 2]. Using his findings, he designed a perforated windscreen which used the pressure and phase differences around the sphere to minimize the

pressure at its center (where the microphone diaphragm would be). Unfortunately, this technique is only valid for unidirectional flow, and no similar closed-form solution seems possible with omnidirectional boundary conditions. Later, Bleazy found that the flat-weighted decibel noise attenuation, NR, achieved by a spherical wire cage is related to the windscreen volume V (in cubic inches, as stated by the source) [Ref. 7]:

$$NR = 6.77 \log V + 10.4 \qquad (1)$$

Bleazy's source of turbulent flow was a paddle wheel, and he found that the above relation held for flow velocities between 2 and 13 m/sec. Though this result may not be directly applicable to all windscreens, it does reflect a well-accepted principle that noise attenuation is improved by larger windscreens.

Acoustical-component modeling, using empirically determined values for the acoustic impedances of screening membranes and dead air spaces, has also been suggested. One such paper is by Bauer [Ref. 8]. In practice, these models have proved most successful in *post facto* descriptions of measured behaviour and as yet do not represent a truly effective predictive tool. The designs presented later use a mixture of mathematical and experimental methods.

Strasburg [Ref. 9] has recently shown that induced wind noise from spherical and cylindrical wind screens can be represented by a single curve if plotted in terms of the dimensions spectral density ($fS\rho^2V^2$) and the dimensionless frequency (fD/V) where f is the frequency, D is the screen diameter, ρ is the fluid density, V is the wind speed and S is the spectral density of the wind noise at frequency f.

A number of materials have been suggested for use as windscreening membranes. The earliest screens consisted of a fine layer of woven cloth [Ref. 10, 11]. Since then, similar designs have replaced the cloth with wire mesh. Increasingly, balls of reticulated polyurethane foam with a small opening for the microphone have been put to use. In theory, each material has its own advantages and disadvantages. Practically, cloth lends itself best to windscreen fabrication since it is flexible and easy to cut and sew. It does require a frame for support, however, and it is not as durable as wire mesh or foam. Wire screens do not need a great deal of support, but they are prone to denting, a problem that may introduce spurious turbulence of its own. Foam is both durable and easy to use, and it has the added advantage that due to its low density it is acoustically transparent even in considerable thicknesses. One of its greatest possible drawbacks is that, according to Beranek, it has a finite acoustic reactance [Ref. 12]. This could distort an

impulse signal. Also, it can get soaked with rain and then freeze solid, or a snow covering can melt during the day and then freeze at night.

The foam most often used (and used here) for microphone windscreens is flexible, reticulated polyurethane foam. An exothermic reaction of these liquids causes the production of foam–that is, dodecahedral bubbles of controllable, relatively uniform size. Initially, the foam is "closed-pore" in that the bubbles are sealed. Through a chemical or thermal process called reticulation, the walls of these bubbles can be removed, leaving only a skeletal framework which is 97 percent empty space [Ref. 13]. (Thermal reticulation was used for the "Scott Industrial Foam" used in these experiments.)

At typical audio frequencies of 100 to 5000 Hertz (Hz), windscreening using all of the above materials, particularly foam, has been fairly successful, and most recent improvements have been in the realm of aesthetics and durability. However, empirical data in this and other studies show that the peak of the power spectral density of wind noise is well below 100 Hz—in fact, typical peaks are in the vicinity of 30 Hz or below. Unfortunately, these are exactly the frequencies at which blast noise has most of its energy [Ref. 1]. This overlap makes the problem of windscreening for blast noise monitoring much more difficult than that for more typical audio signals.

A well-accepted expression for the theoretical frequency content of intrinsic atmospheric turbulence is that derived by Davenport [Ref. 14]:

$$\frac{\eta S(\eta)}{\beta^2/\upsilon} = \frac{(\eta L/\bar{v})^2}{[1+(\eta L/\bar{v})^2]^{4/3}} \tag{2}$$

where

η	is the frequency of turbulence
$S(\eta)$	is the spectral density of turbulence; and
$\bar{v}$, β^2/υ, and L	are empirically determined constants characteristic of the wind.

For large n (and beyond the source region), the expression becomes

$$S(n) \propto n^{-5/3} \tag{3}$$

or, taking the log of both sides,

$$\log S(n) \propto -\frac{5}{3}\log(n) \tag{4}$$

Thus, a log-log plot of the spectral density versus frequency will show a linear relationship at high frequencies with a slope of -5/3. Experimental evidence tends to agree with this formulation, though the spectral peak of

the turbulence varies proprotionally with distance above the ground. According to Duchene and Marullaz, the peak can be as low as 0.03 Hz at heights above 100 m, though at the heights of approximately 1 m used here the peak is closer to 5 or 6 Hz [Ref 15]. It should be clear from these numbers that intrinsic turbulence is primarily a low-frequency phenomenon.

As stated earlier, inserting a microphone into this already turbulent flow compounds the problem. A windscreen can smooth out the intrinsic turbulence, but it introduces turbulence of its own which may be just as troublesome. Wake turbulence is produced by the air which is diverted by the body of the windscreen and then flows back into place on the leeward side. The eddies here have greater characteristic lengths and are therefore responsible for most of the low-frequency screen-induced noise a microphone detects.

These classical principles were well quantified by Reynolds [Ref. 16]. The flow patterns set up by any object in a fluid stream are characterized by the Reynolds number,

$$Re = \bar{\rho}\,\bar{v}\ell/\mu \tag{5}$$

where

Re is the Reynolds number,

$\overline{v}$ is the mean flow velocity,

μ in the fluid viscosity,$1.98 \times 10^{-5} kg/m - sec$ for air,

ρ is the fluid density, $1.18 kg/m^3$ for air; and

ℓ is the characteristic length of the perturbing object.

Over a broad range of Reynolds numbers ($250 < Re < 10^5$), which includes most of the situations encountered here ($6 \times 10^4 < Re < 3 \times 10^5$), the flow pattern is a series of oscillating vortices behind the object (the "wake").

The fundamental frequency, f at which this "vortex shedding" occurs is given in terms of the Strouhal number,S. The Strouhal number is dependent on the shape and surface roughness of the object. For a (hard) sphere in this range of Reynolds numbers, $S \simeq 0.18$, which would indicate a vortex shedding frequency of 2 to 8 Hz for a conventional foam-ball windscreen in a typical flow with velocities in the 2 to 8 m/sec range [Ref. 17]. (The foam is *not* hard, but as an approximation it may be taken as such.)

There is one more mechanism that affects the windscreen-induced turbulence. On the leeward side of the screen, the emerging through-flow helps to annul the region of low pressure which is normally found there. This discourages wake vortices from curling in close behind the screen, thereby

reducing the total intensity of the wake turbulence and also further removing it from the vicinity of the microphone. Unfortunately, the technique of increasing porosity cannot be carried to the limit; that is, the porosity cannot be made so low that the airstream is not blocked at all. The problem of low-frequency windscreening is to block as much flow-through as possible while still minimizing wake effects.

Experimental evidence in this regard has been provided by Hosier and Donovan, whose results are in agreement with this hypothesis [Ref. 18]. In particular, Figures 2 and 3 compare the windnoise reduction of two polyurethane foam spherical windscreens identical except in porosity, measured in pores per (linear) meter, or ppm [Ref. 1]. The screen with a lower porosity (larger holes) shows less noise reduction overall, especially at higher frequencies, but below 100 Hz it shows approximately a 6 dB improvement. In terms of the flow-through/wake hypotheses, this can be interpreted as follows: larger holes permit more air to flow through the membrane and divert less of it. Therefore, more of the windnoise is the flow-through (high-frequency) variety, and less is the wake (low-frequency) variety.

A very successful technique for blocking flow-through was demonstrated by Ballard and Izquierdo in an original paper on the topic of layered windscreens [Ref. 20]. They showed, first theoretically and then experimentally,

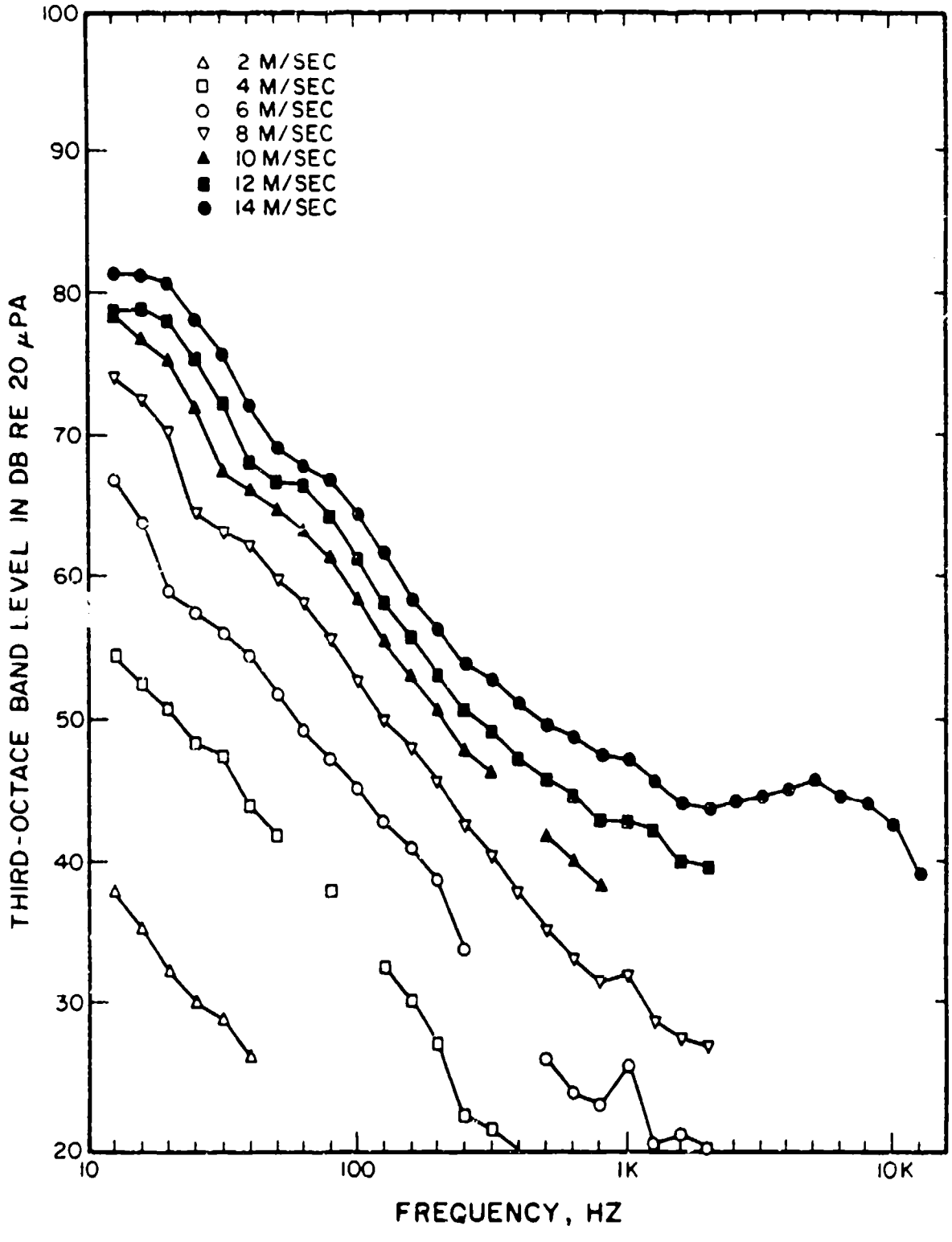

Figure 2. Windscreening performance of a high-porosity (2200) ppm) foam ball. [Ref. 19]

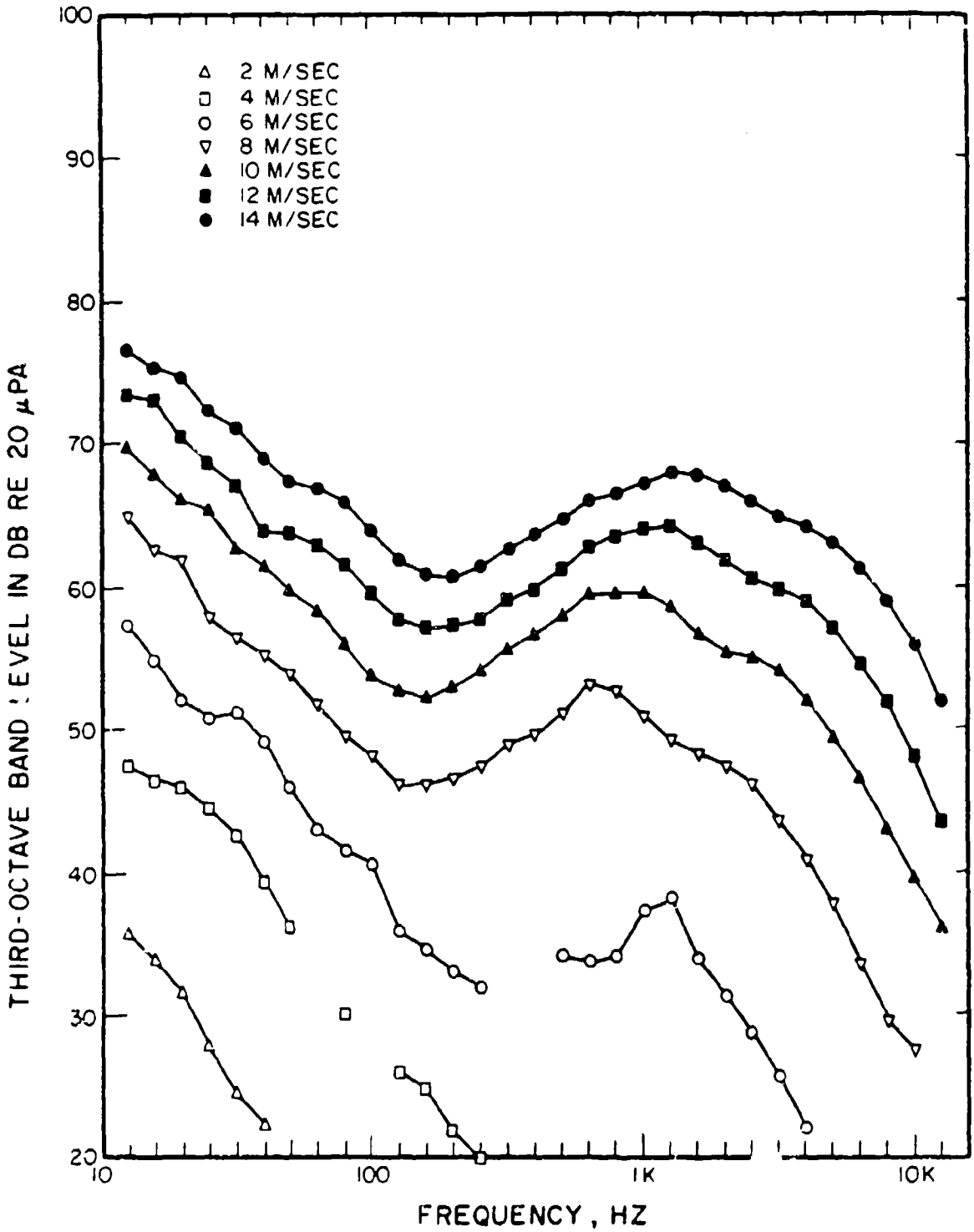

Figure 3. Windscreening performance of a low-porosity (500 ppm) foam ball. [Ref. 19]

that the energy in flow-through airstreams can be dissipated effectively by the use of successive layers of windscreening membranes. Their most important observation was that for small Reynolds numbers, the Navier-Stokes equation for an incompressible fluid becomes

$$\mu \nabla^2 \bar{v} - \nabla P = 0 \tag{6}$$

where

μ is the coefficient of viscosity,

$\bar{v}$ is the fluid velocity, and

P is the fluid pressure.

This implies that the flow pattern (as described by $\nabla^2 \bar{v}$) is dependent on the viscosity of the medium, which in turn implies the dissipation of energy in the form of viscous heating.

It is known that the amount of viscous heating in a fluid is inversely proportional to the size of the velocity gradients in the turbulence. Furthermore, large velocity gradients are associated with small eddies. Ballard and Izquierdo demonstrated that the small eddies set up by a screen cause the dissipation of turbulent energy. Though the screen may not actually block

the flow, it smooths it out and reduces its velocity. A second screen, spaced sufficiently far away, encounters lower flow velocities and reduced turbulence, making its task much easier. The process may be repeated with even more layers. If the above flow-through/wake hypothesis is correct, this layering technique should work exceptionally well for low-frequency windscreening because the flow-through is dissipated and therefore is *not* diverted into the wake.

The relationship between the pressure at the microphone and the flow velocity is given by Bernoulli's principle [Ref. 21],

$$P = \frac{1}{2}\rho v^2 + (\text{potential terms}) \tag{7}$$

Differentiating, one finds that

$$dP \propto v dv, \tag{8}$$

where dP gives some measure of the pressure variations involved. In atmospheric measurements, Daigle has observed that a reduction in flow velocity results in a reduction of flow velocity fluctuations [Ref. 22]:

$$v \propto dv, \tag{9}$$

Together, these results give

$$dP \propto v^2. \tag{10}$$

Thus, a windscreen which reduces flow velocity by a factor of 10 might be expected to reduce turbulence by a factor of 100.

It is notable that Ballard and Izquierdo considered only wire mesh as a screening membrane. Whereas the fluid dynamics governing mesh are much more tractable, it is probable that foam, by its very nature (a three dimensional gridwork), should improve upon the dissipation characteristics of a layered screen. The lattice would force the formation of small eddies and thereby increase viscous losses. The question of how such a screen might best eliminate *wakes* (vortex shedding) will be taken up shortly.

To test the above theoretical predictions, and to develop an optimal layered-foam configuration, a number of tests were conducted on foams and wire/foam combinations.

In order to reliably evaluate the performance of many different windscreen configurations, it is necessary to use a controlled source of airflow. Outdoor measurements, though commendable for their realism, cannot be considered controlled in the scientific sense of the term, due to the variability of outdoor wind. Many researchers have used either wind tunnels

or rotating booms to achieve a uniform flow on which to base their experiments. Both achieve high reproducibility in terms of incident flow and for that reason provide some satisfactory experimental data. Unfortunately, the "wind" produced in either of those arrangements—particularly in the wind tunnel—is not at all characteristic of real outdoor conditions. The wind tunnel restricts flow to the sides, and both methods are characterized by unrealistically uniform flow.

For these tests, two different wind sources were chosen. These offer some advantages over the two methods mentioned above. As a source of uniform flow and measurable flow velocity, a forced-air source was used as illustrated in Figure 4. The flow velocity at various distances from the source was measured with a hot-film anemometer. In the absence of obstructions, the windspeed decreased with a dependence of approximately $1/r$, where r was the distance from the source. Although this cannot be considered a constant flow, such as a wind tunnel produces, it is well-defined and reproducible, and the effects of an interposed membrane can be measured meaningfully.

Recognizing the importance of turbulence inherent in outdoor wind even in the *absence* of an obstruction such as a windscreen, i.e., intrinsic turbulence, tests were also performed with a turbulent source—a 37 cm electric blade fan. The airflow produced by the fan suffered in the scientific sense

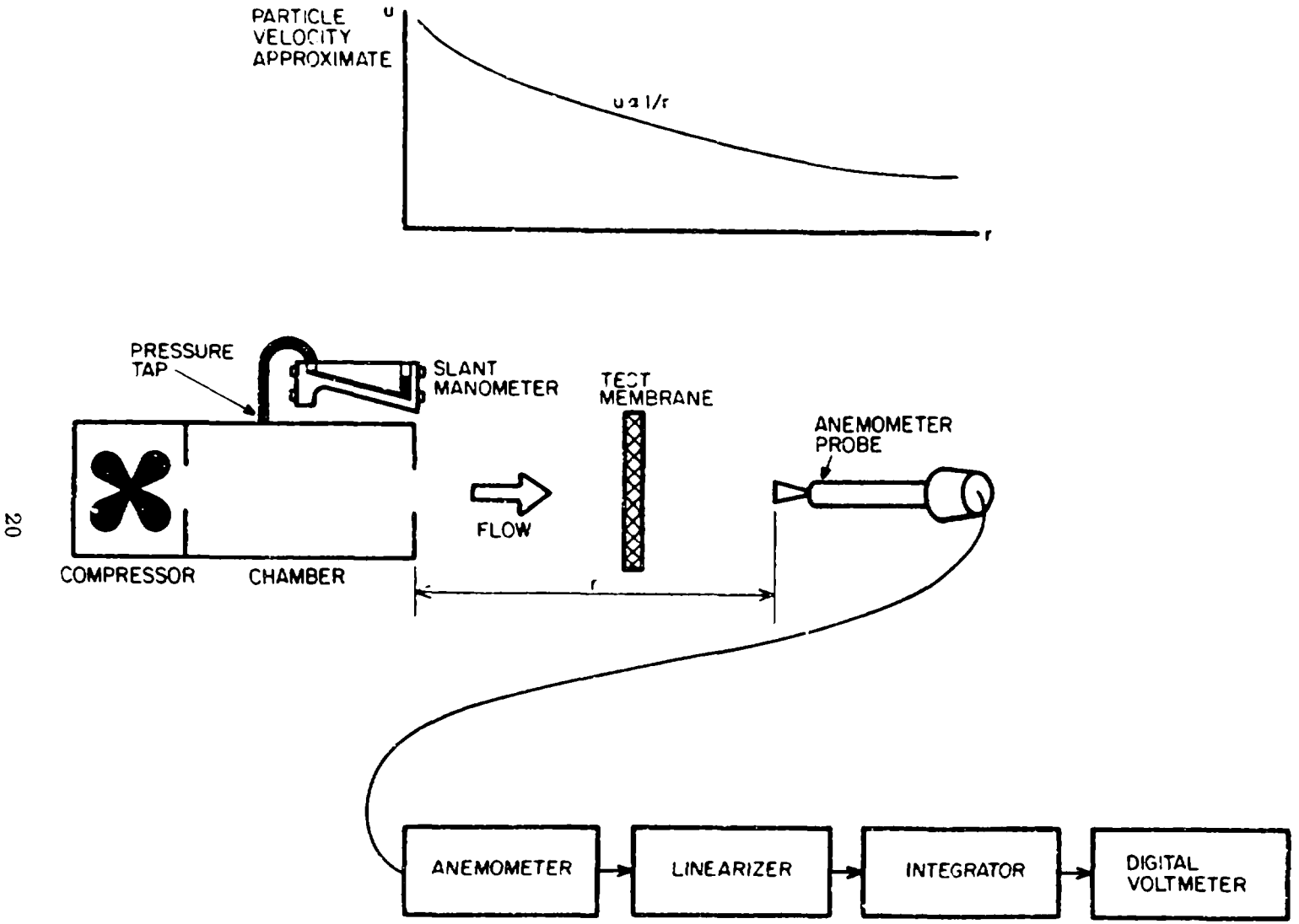

Figure 4. Forced air source.

from its lack of uniformity. Flow velocity, for example, was difficult to measure. However, with careful positioning in front of the fan, the time-averaged windnoise levels recorded by an *un*screened microphone over a sufficiently long sampling period were very repeatable. The fan used had several different speed settings, so screens could be tested under varying, but controlled, turbulent wind conditions.

Using the two techniques above, the performance of numerous windscreening membranes and combinations thereof was tested. Some of the more significant results are tabulated in Tables 1 and 2, and Figures 5 and 6 show plots of portions of the data. These figures demonstrate that wire mesh of 1180 ppm blocked about the same amount of wind as 1.3 cm of 400 ppm foam or about 0.9 cm of higher density foams. The blocking capacity of foam increased with thickness in an approximately linear manner up to a thickness of 2.5 cm, where the wind reduction leveled off. (Note that this occurred under limited flow velocities. It may be that the limiting thickness increases with increasing flow velocity. Also note that the maximum velocities in these experiments were near the high end of typically observed outdoor windspeeds, about 9.6 m/sec.) By measuring the flow velocity at various distances from the membrane on the leeward side, it was found tht windspeed reached a minimum at approximately 17 cm from a foam layer

Table 1

Windspeed as a Function of Distance-- Forced-Air Experiment

Note: The windspeed data represent an arbitrary scale where 100 corresponds to about 9.6 m/s. All values are ± about 20 %. These data are plotted in Figure 6.

Distance(cm)	30	32	35	40	45	50
No Screen	40	38	34	30	25	23
	70	66	60	52	45	41
	100	94	85	75	65	58
1180 ppm	40	9.0	8.4	7.0	6.8	6.6
mesh	70	17	16	12	—	10
	100	24	21	20	18	16
0.3 cm	40	20	17	15	15	14
400 ppm	70	36	31	28	27	26
	100	51	44	40	44	38
0.6 cm	40	9.4	8.2	7.2	7.0	6.8
400 ppm	70	19	16	14	13	—
	100	25	22	20	20	17
2.5 cm	40	5.3	4.5	4.2	—*	—*
400 ppm	70	9.1	8.2	7.2	5.4	4.9
	100	13	11	9.0	7.2	7.2
3.8 cm	40	—	—	—	—	—
400 ppm	70	6.8	6.5	5.8	5.4	4.2
	100	9.1	8.8	8.0	7.5	7.2
0.3 cm	40	—	—	—	—	—
3200 ppm	70	17	15	14	12	11
	100	23	20	18	17	16

*Flows here are too low to be measured reliably.

Table 2

Results of Turbulent-Source Experiment

Note: The microphone is always 41.2 cm from the source. The conditions include various combinations of foam ball windscreens and flat panels of foam placed at the distances noted between the source and the microphone.

	10 Hz	20 Hz	100 Hz	1000 Hz	Overall
No Screen 41.2cm	106.8	104.9	95.9	73.5	112.2
A	(38.4) 68.4	(37.3) 67.6	(16.7) 79.2	(1.9) 71.6	(28.2) 84.0
B	(5.1) 101.7	(2.5) 102.4	(0.0)* 95.9	(0.0)* 73.5	(0.0)* 112.2
C	(21.1) 85.7	(25.1) 79.8	(12.1) 83.2	(-1.5) 75.0	(23.8) 88.4
D	(23.9) 82.9	(21.5) 83.4	(15.2) 80.7	(0.2) 73.3	(29.8) 87.4
E	(31.1) 75.7	(32.6) 72.3	(15.3) 80.6	(0.4) 73.1	(25.2) 87.0
F	(32.8) 74.0	(33.9) 71.0	(15.6) 80.3	(1.4) 72.1	(27.0) 85.2

*The zeros of "B" are not absolute—they merely indicate a speed too small to measure.

Levels in dB
Reductions compared to unscreened levels are shown in parentheses.
The Microphone is always 41.2 cm from source:

A: 17 cm diameter 1200 ppm foam ball, 2.5 cm thick 400 ppm panel at 15.8 cm from the source
B: 2.5 cm thick 400 ppm foam panel at 15.8 cm from source only
C: Foam ball only
D: Foam ball, 2.5 cm thick 1180 ppm panel at 15.8 cm from the source
E: Foam ball, 2.5 cm thick 400 ppm panel adjacent to foam ball
F: Foam ball, 2.5 cm thick 400 ppm panel at 26.7 cm from source

Note: Other spacings were also investigated.

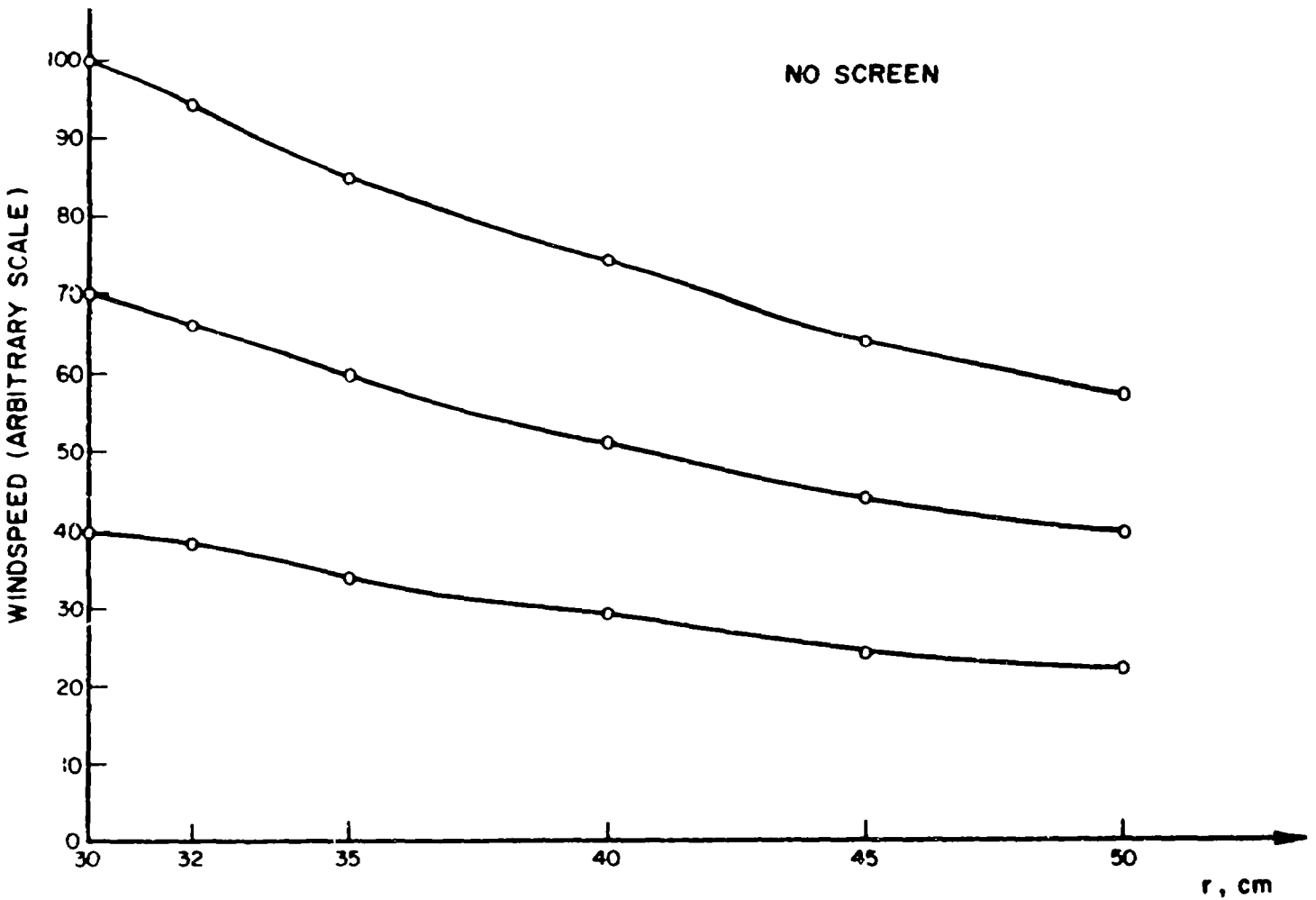

Figure 5. Windnoise levels recorded by an unscreened microphone.

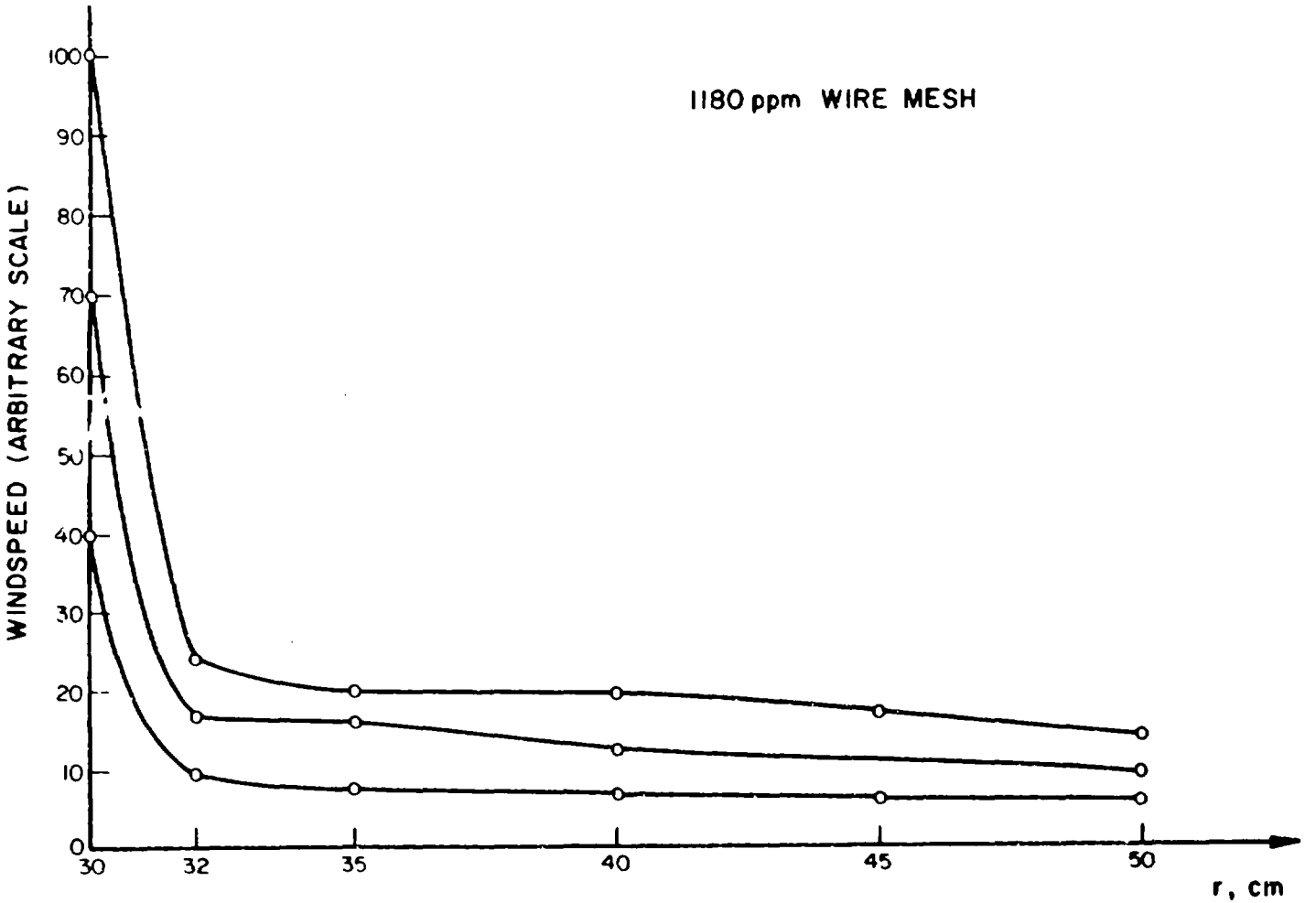

Figure 5. (Cont'd)

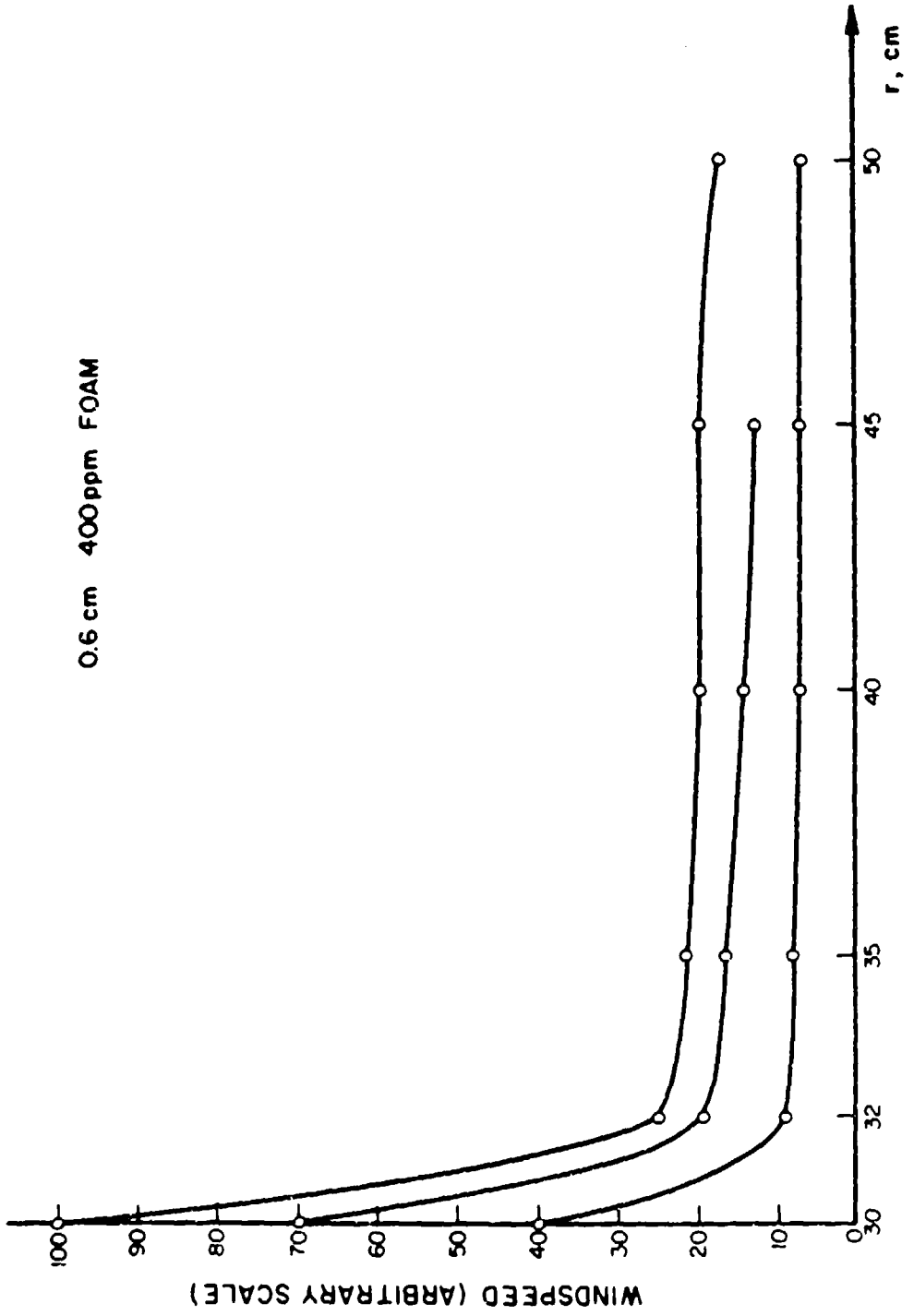

Figure 5. (Cont'd)

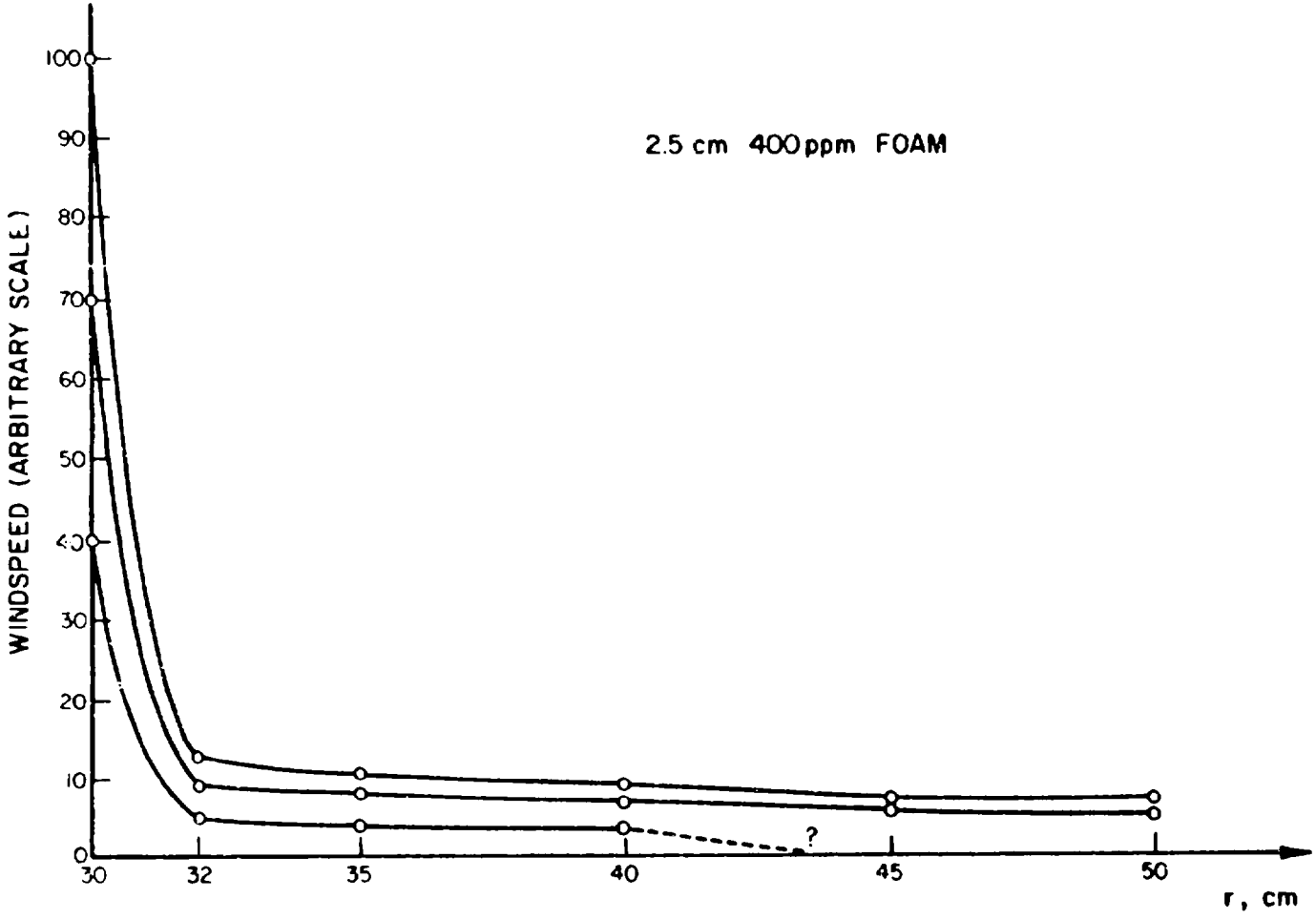

Figure 5. (Cont'd)

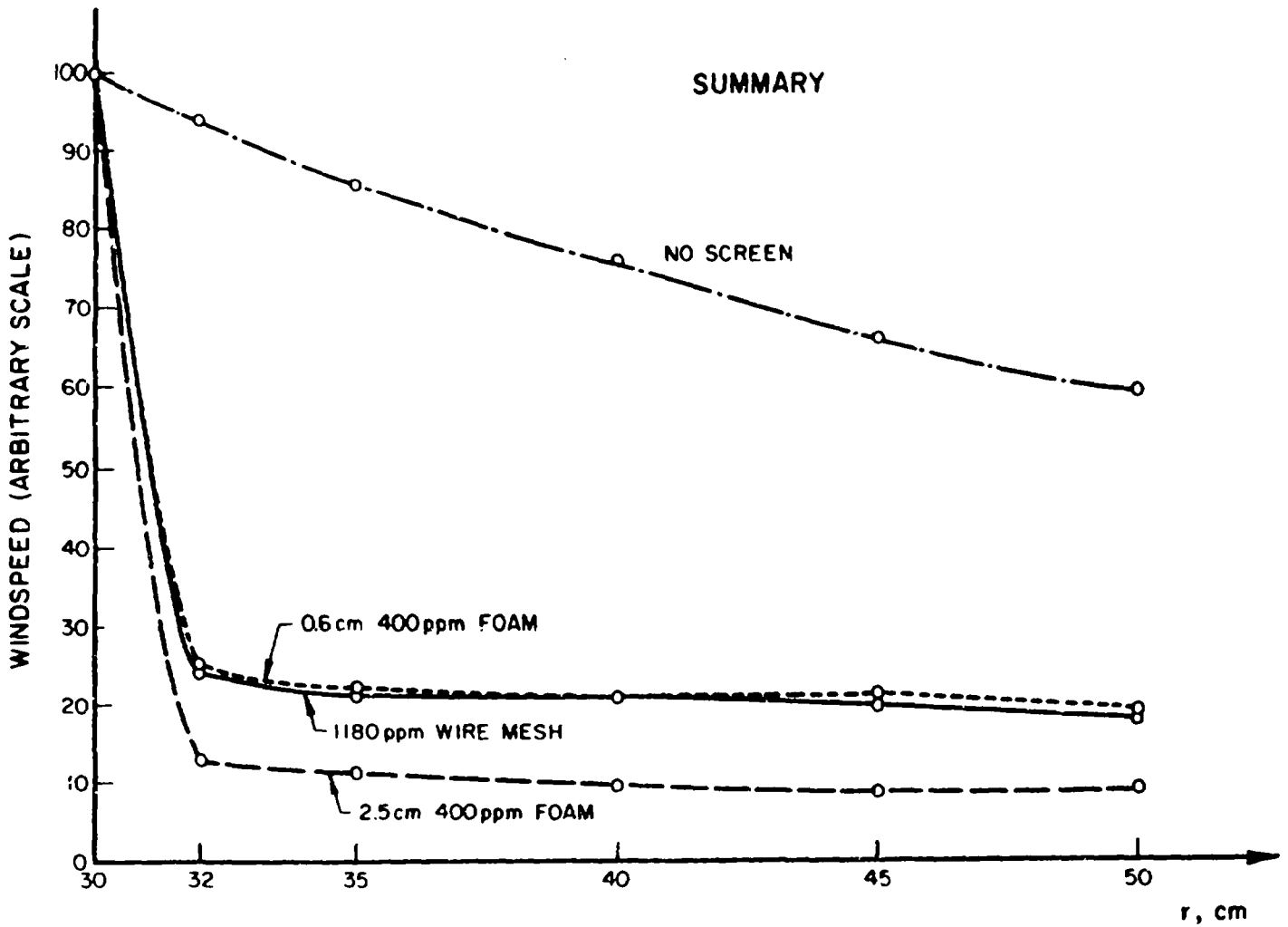

Figure 5. (Cont'd)

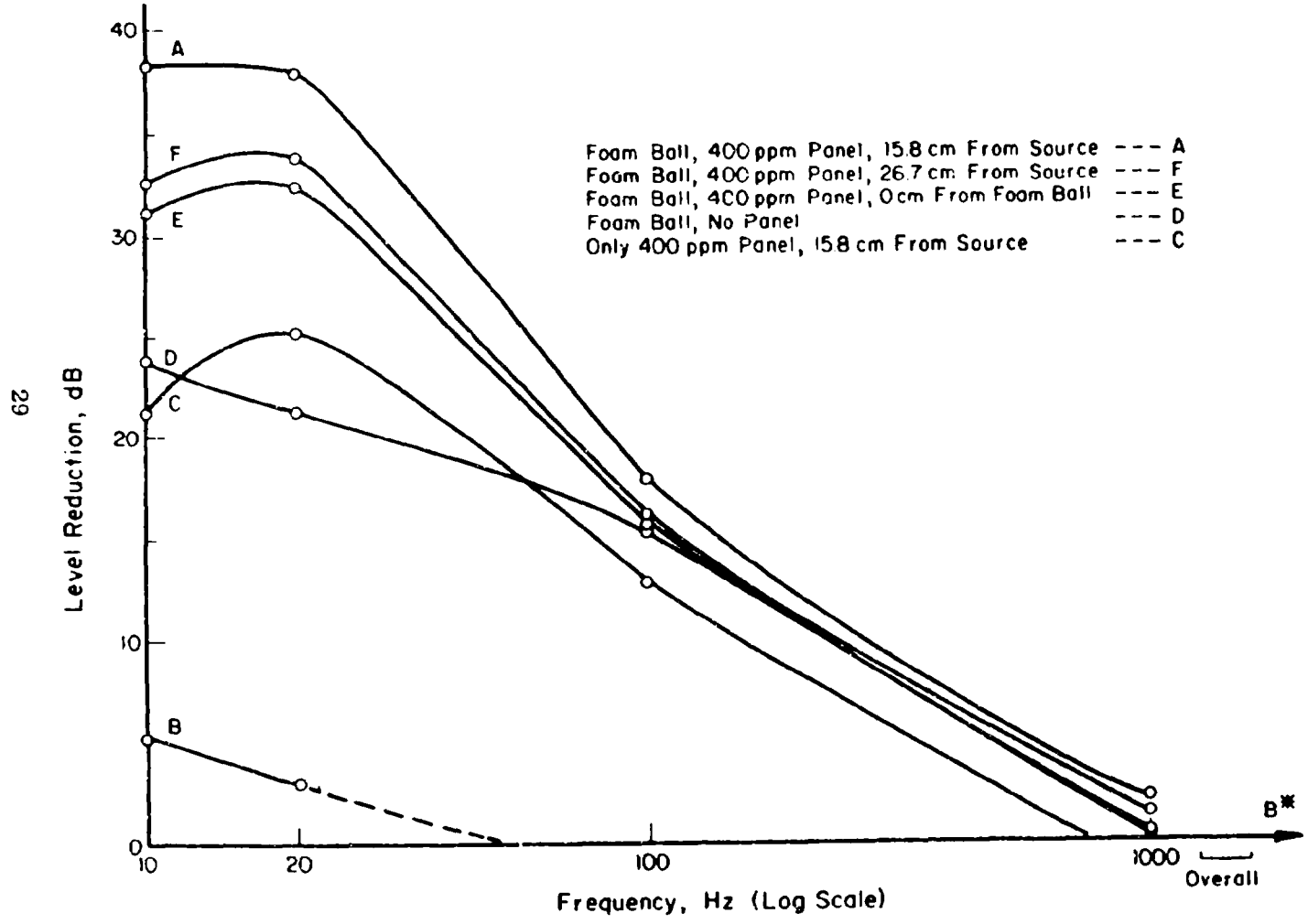

Figure 6. Turbulent source membrane performance.

2.5 cm thick. Beyond that distance it remained approximately constant, though effects from wind flowing around the screening membrane caused some small-scale turbulence at greater distances. Under low-wind conditions, the most effective screen available was a foam ball of 17 cm diameter. Using the combined results, it was found that very effective flow-through reduction could be achieved in these controlled, simulated outdoor conditions by enclosing the transducer in a 17 cm diameter, 1200 ppm foam ball which was shielded at 17 cm by a 2.5 cm layer of low-porosity (400 ppm) foam. It was possible to achieve similar degrees of noise reduction by repeated use of multiple layers of wire mesh or foam, but this combination proved simplest.

3 MICROPHONE ARRAYS

The Principle of Microphone Arrays

A windscreen is probably the most direct *mechanical* technique for eliminating pseudosound. It is also possible, however, to use electronic *processing* techniques on the signal after it has passed through the microphone transducer. A complete outdoor noise-monitoring system can employ both techniques. In particular, early work done in this study based on earlier concepts by a number of acousticians showed the feasibility and advisability of implementing a multiple-microphone array [Ref. 23-29].

The use of microphones arrays is based on the principle that windnoise (that is, pressure fluctuations due to turbulence), despite its low-frequency characteristics, is very localized, and at some distance, uncorrelated. However, an acoustic signal from some distance away will arrive simultaneously, or nearly so, at two separate microphones which are aligned perpendicular to the direction of acoustic propagation. In the case of blast noise from some distance away, near-ground-level monitoring is practical, so the direction of acoustic propagation is very close to horizontal. With such a situation, it is clear that the microphones should be spaced vertically; one might be perhaps a few meters off the ground, pointing up, and the other would be, for

example, 50 cm above it, pointing down. This allows for omnidirectional sensitivity in the horizontal plane, and it also ensures that blasts will arrive coincidentally at each microphone.

In the initial studies for the particular case of blast noise, it was observed that there is often a recognizable peak whose time of arrival can be determined at each microphone. If the difference between the two times of arrival is small, then the event can be interpreted as a blast. If it is not small, or if the size of the peaks detected at each microphone is very different, then the event can be interpreted as windnoise. However, subsequent studies showed that: (1) the time-of-arrival of the peak is a difficult quantity to measure accurately, and (2) better wind noise rejection can be accomplished by considering the entire blast and not just the peak.

This approach to the problem of wind noise reduction, i.e., considering the entire blast, was suggested by Buck and Greene's method for reduction of non-acoustic noise in underwater sound measurements [Ref. 29]. This method is based on the reasonable assumption that the phenomena responsible for non-acoustic pressure variations $n(t)$ will be uncorrelated at points sufficiently separated in the wave conducting medium (water or air). Thus, for two sufficiently separated pressure transducers,

$$\overline{n_1(t)n_2(t)} = 0 \tag{11}$$

If the distances from an acoustic source to the two transducers are nearly equal with respect to a wavelength of the acoustic wave, then the acoustic pressures $p_1(t)$ and $p_2(t)$ received at the transducers will be highly correlated:

$$p_1(t) = p_2(t) = p(t) \tag{12}$$

It is also reasonable to assume that the acoustic and nonacoustic pressures are uncorrelated:

$$\overline{p(t)n_1(t)} = \overline{p(t)n_2(t)} = 0 \tag{13}$$

The net pressure $s(t)$ at the diaphragm of a pressure transducer is the sum of the acoustic and nonacoustic pressures:

$$s(t) = p(t) + n(t) \tag{14}$$

Thus, under the above three conditions, the mean-square acoustic pressure can be recovered from the two transducer signals:

$$\begin{aligned}\overline{s_1(t)s_2(t)} &= \overline{[p_1(t)+n_1(t)][p_2(t)+n_2(t)]} \\ &= \overline{p^2(t)} + \overline{p(t)n_1(t)} + \overline{p(t)n_2(t)} + \overline{n_1(t)n_2(t)} \\ &= \overline{p^2(t)} \qquad (15)\end{aligned}$$

Practical Considerations in Two-Microphone Arrays

Early in this work, the principles discussed above were applied to the design of a blast detection system to be used in conjunction with a windscreen. The purpose of the system was to distinguish between acoustic blast signals and gusts of wind by comparing the outputs from two microphones. The system output was a binary decision as to the type of signal present. This decision was available for use by other monitoring equipment or to aid in selection of valid data for later analysis.

This early system did not explicitly compute the cross product of the two microphone signals. Rather, when both signals exceeded a preset threshold, the system measured the peak signal levels and their times of arrival at each microphone. These characteristics were then compared: if the peak levels were nearly the same and the difference in peak arrival times (the peak spacing) was small, then the signals were correlated, which indicated an acoustic excitation [Eq. 12]. If the sets of characteristics did not match

up, then a wind gust was indicated [Eq. 11]. The preset threshold served to exclude from consideration signals other than blasts or wind gusts, since in a blast measurement situation other types of signals as large as these two are seldom encountered.

One of the conditions for application of Buck and Greene's technique is that the acoustic source be nearly equidistant from the two microphones with respect to the acoustic wavelength. This may be ensured by positioning the microphones on a line perpendicular to the direction of propagation of the acoustic wave. In blast noise measurement, as in some other situations, the sources of interest are usually at ground level and may be treated as point sources. In this case, as noted above, the condition of equal distances may be satisfied by placing the microphones in a vertical array, as shown in Figure 7. This placement allows omnidirectional reception from ground level sources; signal coherence is assured as long as the difference in path length remains much less than a wavelength, which is almost certain for blast signals since the frequencies involved are so low. This optimum microphone placement was arrived at early in this work and used as a basis for the design of all subsequent windscreens.

A further condition for the valid implementation of a two-microphone wind noise reduction system was revealed by the early studies of blast peak

coincidence at two microphones in a vertical array. In these, the microphones were separated by 55 cm, with the lower microphone about 160 cm from the ground. The nearest blast site was 5.6 km away, so the difference in path length from this site to the microphones (as in Figure 7) was about 0.2 mm. Thus, the expected difference in arrival times of blast peaks at the microphone was 0.6 *s*; but the observed values averaged 3 ms, much longer than could be explained by acoustic propagation phenomena. The cause of

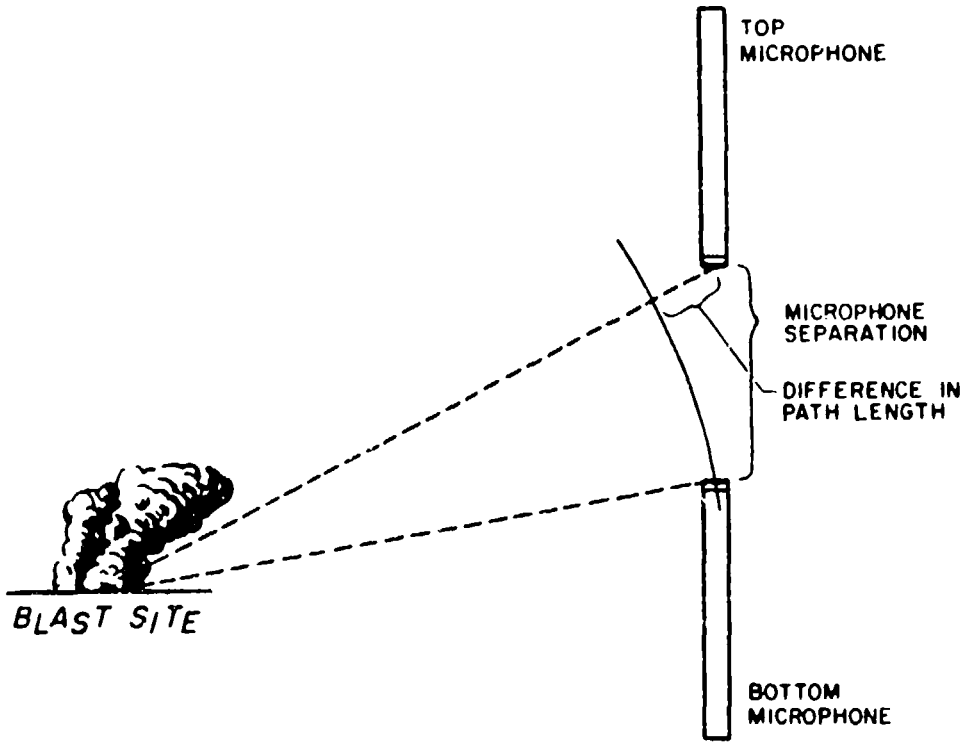

Figure 7. Path length comparison.

this discrepancy turned out to be a difference between the frequency responses of the two microphones. In these early studies, the microphones typically had low frequency corners of 8 to 12 Hz. Assuming a one-pole frequency response (45 degree phase shift at the corner frequency), two microphones with corner frequencies at 9 and 11 Hz will show a 5 degree difference in phase shift at 10 Hz, which implies a time lag of 1.4 ms at this frequency. This is close to the observed difference in blast peak arrival times. Since both blasts and wind noise have much of their spectral energy below 10 Hz, microphones with very closely matched frequency responses are required for any signal correlation measurement to be meaningful.

The early blast detection system was designed to differentiate between blast signals and gusts of wind using the principles inherent in Buck and Greene's techniques, and the system has the advantage of being easily implemented with digital hardware. However, the peak detection requirement clearly and fatally flaws this technique in situations where the blast signals are combined with, or perhaps even buried in, wind noise. In theory, though, Buck and Greene's technique is capable of actively removing the wind noise from the total received signal, leaving just the acoustic signal. In the following text a direct implementation of the technique is introduced which more completely realizes the potential for wind noise reduction.

4 THEORY FOR A TWO-MICROPHONE ARRAY

Basic Theory

The method of Buck and Greene can be applied to two different measures of sound, sound exposure level (SEL), which is symbolized L_E, and the time averaged sound pressure level (LEQ), whose symbol is L_T [Ref. 30], [Ref. 32]:

$$L_E = 10 \log \left[\frac{1}{t_0 p_0^2} \int_0^T p^2(t) dt \right] \quad \text{dB} \tag{16}$$

$$L_T = 10 \log \left[\frac{1}{T p_0^2} \int_0^T p^2(t) dt \right] \quad \text{dB} \tag{17}$$

where $p(t)$ is the acoustic pressure, p_0 is a reference pressure in air of 20 μPa, t_0 is a reference time of 1 second, and T is the period of time over which the pressure is integrated. The LEQ is used as a measure of continuous sounds; SEL is appropriate for transient sounds such as blast impulses. The important difference between the two level definitions is that in computing LEQ the average of the squared pressure is used, while in finding SEL the integrated squared pressure is divided by a constant reference time. Both measures involve the integral of the squared pressure.

The signal $s(t)$ available from a single microphone is acoustic pressure $p(t)$ plus nonacoustic pressure $n(t)$, as in Equation (14). If this signal is

squared, three terms result:

$$s^2(t) = [p(t) + n(t)]^2 = p^2(t) + 2p(t)n(t) + n^2(t) \tag{18}$$

If two microphones are placed so that they receive identical acoustic signals ($p_1(t) = p_2(t) + p(t)$), as described earlier, then the product of their output signals gives four terms as in Equation (15):

$$\begin{aligned} s_1(t)s_2(t) &= [p_1(t) + n_1(t)][p_2(t) + n_2(t)] \\ &= p^2(t) + p(t)n_1(t) + p(t)n_2(t) + n_1(t)n_2(t) \end{aligned} \tag{19}$$

In either case, integration over the measurement interval gives the acoustic pressure term required for the sound level measurement, plus several undesired noise terms; the noise terms are random variables whose properties depend on the sound level calculation being made. A probabilistic analysis of these terms is carried out in the Appendix, and the results are used here to characterize the sound level measurement errors caused by the noise.

Measurement of SEL

To find the SEL, the acoustic pressure must be squared and integrated over the measurement period T. As has just been shown, this term may be obtained, with others, using one or two microphones. Table 3 contains

Table 3

Summary of Results From Appendix for Square Sound Pressures and Products of Sound Pressures

a. One microphone:
(square sound pressures)

$$\int_0^T s^2(t)dt = \int_0^T p^2(t)dt + 2\int_0^T p(t)n(t)dt + \int_0^T n^2(t)dt$$

noise term	mean	variance
$\int_0^T p(t)n(t)dt$	0	$\int_0^T \int_0^T p(t)p(s)R_n(t,s)dtds$
$\int_0^T n^2(t)dt$	$T\sigma_n^2$	$\frac{\sigma_n^4}{b^2}[2bT + \exp(-2bT) - 1]$

b. Two microphones:
(product of sound pressures)

$$\int_0^T s_1(t)s_2(t)dt = \int_0^T p^2(t)dt + \int_0^T p(t)n_1(t)dt + \int_0^T p(t)n_2(t)dt + \int_0^T n_1(t)n_2(t)dt$$

noise term	mean	variance
$\int_0^T p(t)n(t)dt$	0	$\int_0^T \int_0^T p(t)p(s)R_n(t,s)dtds$
$\int_0^T n_1(t)n_2(t)dt$	$T\sigma_n^2\exp(-ad)$	$\frac{\sigma_n^4}{2b^2}[1 + \exp(-2ad)]$ $\times[2bT + \exp(-2bT) - 1]$

Notes:

1. σ_n^2 = variance of $n(t)$.
2. $R_n(t,s)$ = autocorrelation of $n(t)$; $\sigma_n^2(1 - b|t - 2|)$.
3. $1/a$ = correlation length of turbulence; $\cong$ 1.1m[13].
4. $1/b$ = correlation time of turbulence, $\cong$ 1/2 to a few seconds (varies with wind speed) [14].
5. T = sound level measurement period.
6. d = microphone separation.

a summary of the equations and noise error term statistics involved here. The noise terms of the form $\int_0^T p(t)n(t)dt$ are relatively insignificant; their mean is zero, and since the acoustic pressure $p(t)$ is a zero mean function (capacitive coupling of the microphones was used to ensure this), the variance of these terms will be small. However, the term $\int_0^T n^2(t)dt$ encountered in the one-microphone case has nonzero mean and variance, and so represents a possibly significant measurement error. The corresponding term in the two-microphone case, $\int_0^T n_1(t)n_2(t)dt$, has a similar nonzero mean; but in this case the mean can be made as small as necessary by increasing the microphone separation d. This term has a somewhat smaller variance also. Thus two microphones can be used to reduce the wind noise error incurred in making a SEL measurement. The dependence of the means and variances on the measurement period T is of little consequence since the length of a SEL measurement will be determined by the length of the transient signal involved.

Measurement of LEQ

To find the LEQ, the squared integrated pressure is divided by the measurement period T. The resulting noise error term statistics are shown in Table 4. Again the terms of the form $\frac{1}{T}\int_0^T p(t)n(t)dt$ are negligible, vanishing completely as T goes to infinity. The term $\frac{1}{T}\int_0^T n^2(t)dt$ in the

Table 4

Summary of Results From Appendix for Mean-Square Sound Pressures and Mean of Product of Sound Pressures

a. One microphone:

$$\frac{1}{T}\int_0^T s^2(t)dt = \frac{1}{T}\int_0^T p^2(t)dt + \frac{2}{T}\int_0^T p(t)n(t)dt + \frac{1}{T}\int_0^T n^2(t)dt$$

noise term	mean	variance
$\frac{1}{T}\int_0^T p(t)n(t)dt$	0	$\frac{1}{T^2}\int_0^T\int_0^T p(t)p(s)R_n(t,s)dtds$
$\frac{1}{T}\int_0^T n^2(t)dt$	σ_n^2	$\frac{\sigma_n^4}{b^2T^2}[2bT + \exp(-2bT) - 1]$

b. Two microphones:

$$\frac{1}{T}\int_0^T s_1(t)s_2(t)dt = \frac{1}{T}\int_0^T p^2(t)dt + \frac{1}{T}\int_0^T p(t)n_1(t)dt + \frac{1}{T}\int_0^T p(t)n_2(t)dt + \frac{1}{T}\int_0^T n_1(t)n_2(t)dt$$

noise term	mean	variance
$\frac{1}{T}\int_0^T p(t)n(t)dt$	0	$\frac{1}{T^2}\int_0^T\int_0^T p(t)p(s)R_n(t,s)dtds$
$\frac{1}{T}\int_0^T n_1(t)n_2(t)dt$	$\sigma_n^2\exp(-ad)$	$\frac{\sigma_n^4}{2b^2T^2}[1+\exp(-2ad)]\times[2bT + \exp(-2bT) - 1]$

Notes

1. σ_n^2 = variance of $n(t)$.
2. $R_n(t,s)$ = autocorrelation of $n(t)$; $\sigma_n^2(-b|t-2|)$.
3. $1/a$ = correlation length of turbulence; $\cong 1.1m$[15].
4. $1/b$ = correlation time of turbulence; $\cong 1/2$ to a few seconds (varies with wind speed) [16]
5. T = sound level measurement period.
6. d = microphone separation.

one-microphone case has nonzero mean and so is a source of error in the LEQ measurement; its variance decreases as T increases, so it could conceivably be measured and removed for very long measurement periods. In the two-microphone case, the mean of $\frac{1}{T}\int_0^T n_1(t)n_2(t)dt$ can be made insignificantly small by using a large enough microphone spacing d, and the variance will become zero as T goes to infinity. Thus, by using the two-microphone method, the error due to wind noise can be completely removed from measurement of LEQ, at least in theory.

The next step in this analysis is to predict the difference between the sound level measured using one microphone and the sound level measured using two microphones, for a given actual sound level and given sets of measurement parameters (measurement period T and microphone spacing d) and noise process parameters (variance σ_n^2, correlation length $1/a$, and correlation time $1/b$). An expression for the single microphone sound level L_S may be obtained by substituting Equation (18) for $p(t)$ in the sound level definition [Eq. 16 or 17]:

$$\begin{aligned} L_S &= 10\log\left[K\int_0^T \{p^2(t) + 2p(t)n(t) + n^2(t)\}dt\right] \quad \text{dB} \\ &= 10\log\left[K\{\int_0^T p^2(t)dt + 2\int_0^T p(t)n(t)dt + \int_0^T n^2(t)dt\}\right] \quad (20) \end{aligned}$$

where $K = 1/Tp_0^2$ for LEQ, or $1/t_0p_0^2$ for SEL. The two-microphone or cross-product sound level L_X is found by substituting Equation (19) for $p(t)$ in the definition:

$$\begin{aligned} L_X &= 10\log[K\int_0^T \{p^2(t) + p(t)n_1(t) + p(t)n_2(t) + n_1(t)n_2(t)\}dt] \\ &= 10\log[K\{\int_0^T p^2(t)dt + \int_0^T p(t)n_1(t)dt + \int_0^T p(t)n_2(t)dt \\ &+ \int_0^T n_1(t)n_2(t)dt\}] \quad \text{dB} \end{aligned} \tag{21}$$

The noise process $n(t)$ in Equation (20) may be equal to $n_1(t)$ or $n_2(t)$ in Equation (21) (but not both). The difference in measured sound levels ΔL is then given by

$$\begin{aligned} \Delta L &= L_S - L_X \\ &= 10\log[K\{\int_0^T p^2(t)dt + 2\int_0^T p(t)n(t)dt + \int_0^T n^2(t)dt\}] - \\ &\quad 10\log[K\{\int_0^T p^2(t)dt + \int_0^T p(t)n_1(t)dt + \int_0^T p(t)n_2(t)dt + \int_0^T n_1(t)n_2(t)dt\}] \\ &= 10\log\left[\frac{\int_0^T p^2(t)dt + 2\int_0^T p(t)n(t)dt + \int_0^T n^2(t)dt}{\int_0^T p^2(t)dt + \int_0^T p(t)n_1(t)dt + \int_0^T p(t)n_2(t)dt + \int_0^T n_1(t)n_2(t)dt}\right] \\ &\qquad \text{dB} \end{aligned} \tag{22}$$

At first it might seem possible to find an expression for the mean of ΔL by substituting the means of the various noise terms from Table 3 into

Equation (22). But this approach is not valid, since the noise terms are not independent; knowledge of their individual means is not enough to find the mean of a quantity which depends on several of the noise terms. In general, prediction of the mean and standard deviation of ΔL is a difficult if not insoluble problem in probability which is beyond the scope of this report. Thus, although the two-microphone calculation is expected to reduce wind noise by an amount that should increase as microphone spacing and measurement period are increased, the exact dependence of the noise reduction on these parameters must be determined empirically.

The results of this section imply that a two-microphone array can be used for direct electronic calculation of the sound level. This system will achieve significant reduction of the turbulent pressure fluctuation interference that affects a one-microphone measurement system. The two-microphone system will effectively reduce wind noise, thus acting as an electronic windscreen. Fairly involved digital processing is required to carry out the two-microphone calculation directly. The calculation is practicable, however, since equipment capable of such processing exists. Examples are the True-Integrating Noise Monitoring and Warning System, Model 370, developed at the U.S. Army Construction Engineering Research Laboratory (USACERL) [Ref. 31] and the Precision Data 6000 computing oscilloscope [Ref. 32]; both instruments sample an input signal and find the SEL or LEQ numerically.

5 TESTING OF THE COMPOUND WINDSCREENS AND MICROPHONE ARRAYS

Testing the Compound Windscreen Design

As noted, the vertical two-microphone array is the configuration around which the windscreen had to be designed. Since symmetry and fidelity of the signals from the two microphones is essential, a windscreen symmetrical about the two microphones is clearly in order. Furthermore, the restraint of omnidirectionality in the horizontal plane imposes a need for radial symmetry as well. Together, these requirements suggest an ellipsoidal or cylindrical design. Traditionally, windscreens have been roughly spherical, presumably to block wind effectively from any direction in all three dimensions. Ballard and Izquierdo tested both a hemispherical screen, which rested on the ground, and a cylindrical one. They preferred the hemisphere, but other investigators have shown that spherical screens are no more effective in windnoise reduction than are cylindrical ones [Ref. 33]. For this study, the modified cylindrical configuration used in the early studies was adopted.

The protected-ball configuration developed in the initial experiments (described in **Windscreens**, above) was easily adapted to cylindrical form. The two vertically spaced microphones were supported by flat plywood

plates are each end of the cylinder, and the 1200 ppm foam balls mentioned above were fitted over the ends of the microphones. The entire arrangement was then wrapped with a 2.5 cm layer of 400 ppm foam at a 17 cm radial distance from the outside of the balls. The screen is illustrated in Figure 8.

The outer layer, consisting of a fairly thick but low-porosity foam, discouraged wake turbulence in three ways. First, its relatively rough surface presented a large Strouhal number and thus hindered low-frequency vortex shedding. Furthermore, its large holes allowed a reasonable amount of flow-through into the outer regions of the screen, thereby dispelling even more flow-around. Finally, it allowed flow out of the leeward side, thereby reducing wake turbulence through the mechanism described in Chapter 1. The layer was thick enough, however, to dissipate a large amount of the incident turbulence. The inner "layer," or ball, was of higher porosity and greater thickness. Its smaller holes blocked the now smoother flow by achieving the large velocity gradients recommended by Ballard and Izquierdo. Wake effects around this ball, thanks to the upstream flow-reduction and downstream vortex disruption of the outer layer, were minimal. Empirically it was found that introducing additional layers between these two (or even outside them) produced no noticeable improvement in windnoise reduction. This result is not in perfect agreement with Bleazy's result that attenua-

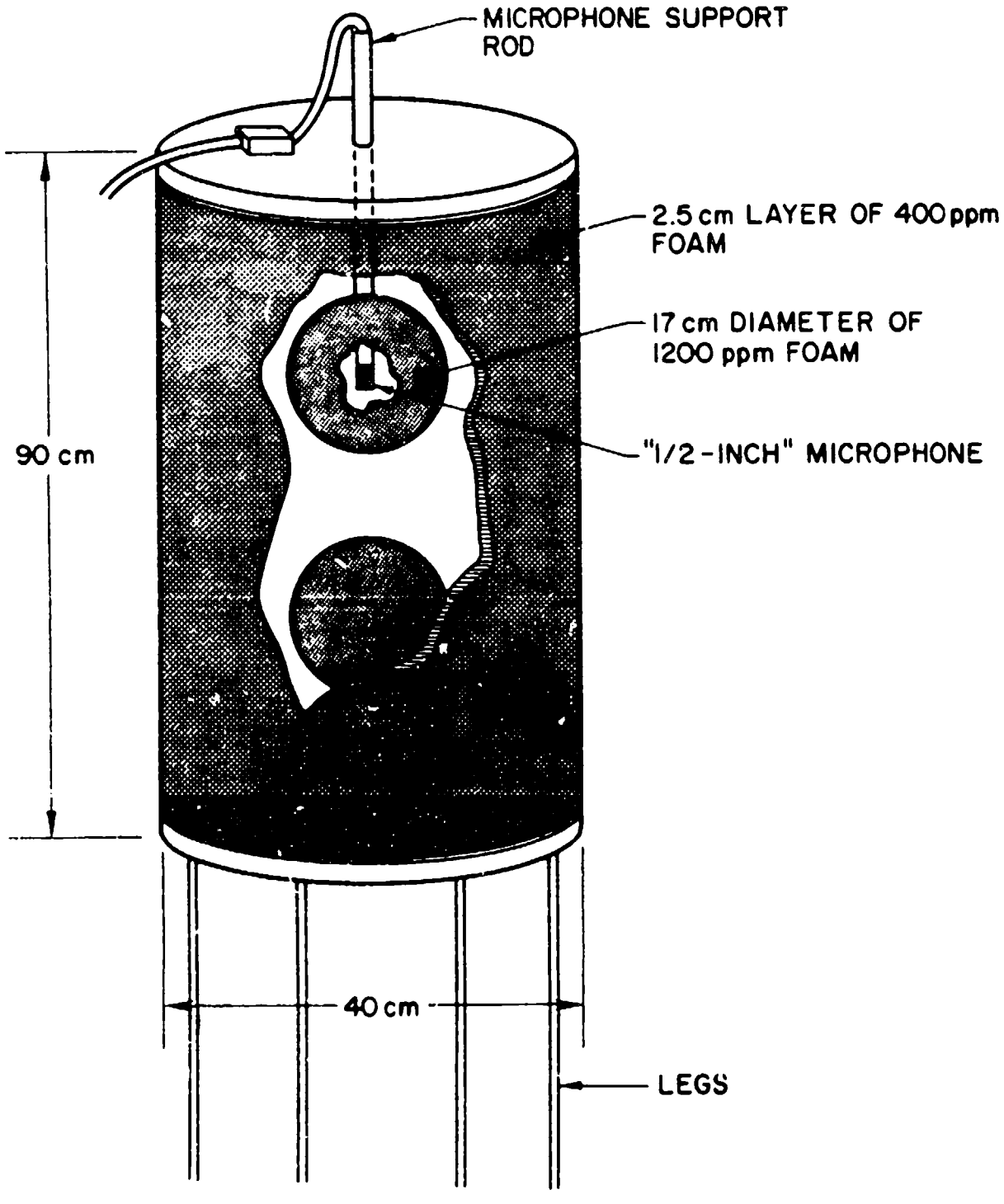

Figure 8. Protected-ball windscreen.

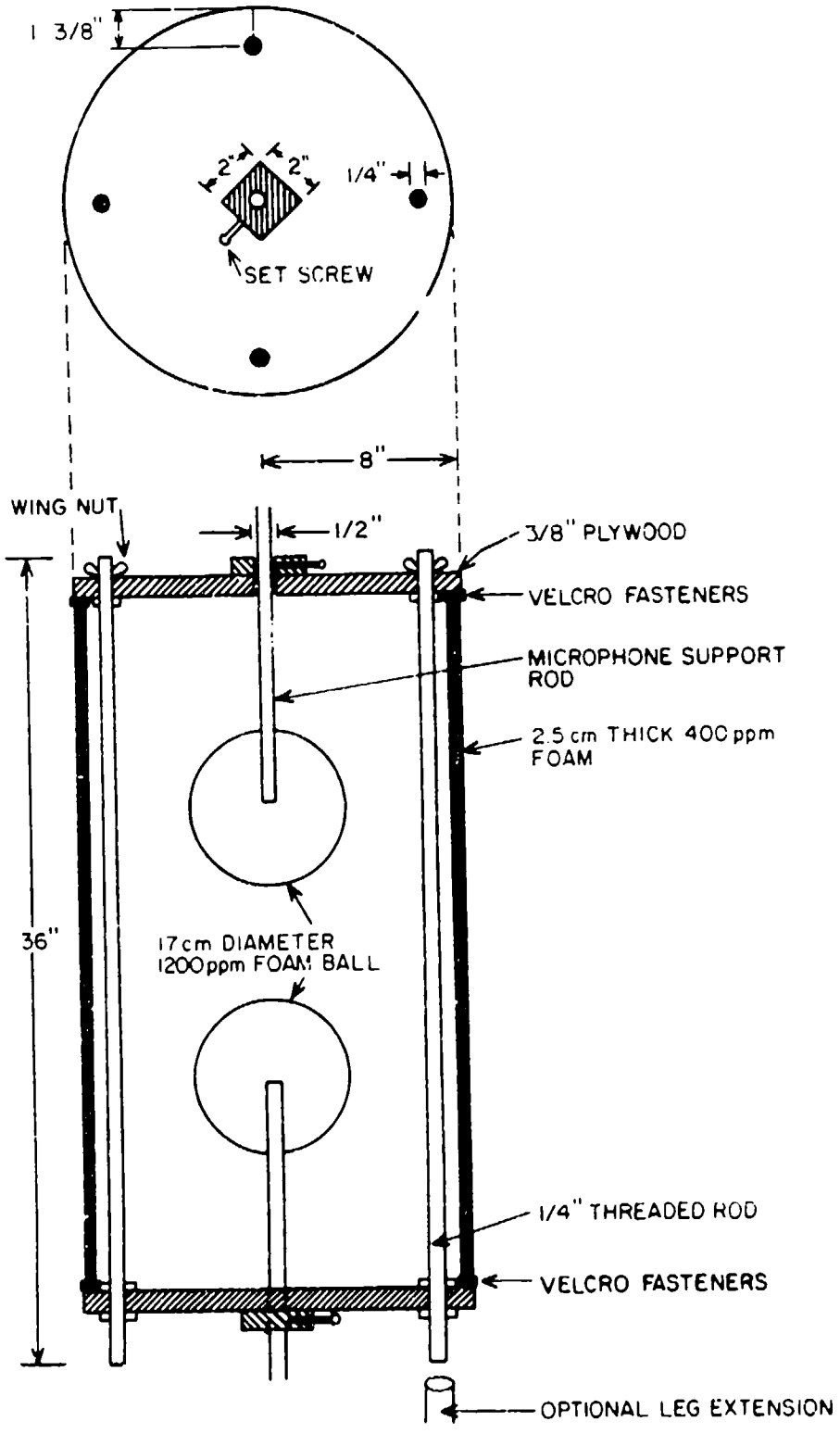

Figure 8. (Cont'd)

tion goes up with size, but it y probable that some limiting level of turbulence-reduction had been achieved with this screen.

In particular, the argument above [Eq. 10] indicates that turbulence drops very quickly with reductions in flow velocity, so in the case of this windscreen, one might expect both the flow velocity and the turbulence to be well-reduced after the first layer of foam. Additional layers encounter low incident flow velocities and therefore can produce only very small relative flow reductions and, consequently, small turbulence reductions. In fact, the minor self-induced turbulence of the foam might be expected to equal or exceed the remaining turbulence intrinsic to the flow. Thus, the layered screen reaches a certain level of reduction saturation.

In an effort to examine the validity of this design, a simple flow-visualization experiment was conducted. In it, a windscreen with one end removed and replaced by Plexiglas was set up at the mouth of a wind tunnel. Smoke streamers were introduced into the flow, and the smoke's progress through and past the windscreen was photographed. The experimental setup and some of the results are shown in Figure 9. It can be seen that the screen performed largely as predicted above. The incident flow was slightly turbulent, but it smoothed out considerably as it passed through the first layer of foam. Measured particle velocities dropped over 40 percent, going from

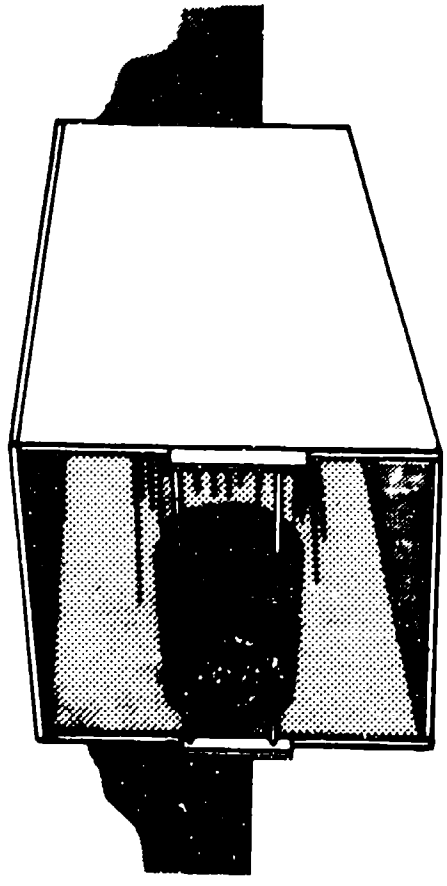

Figure 9a. Flow-visualization experiment setup.

Figure 9b. Turbulent smoke streamer (lower center) flows into screen (left).

Figure 9c. Smooth flow inside screen (flow direction is from right to left).

Figure 9d. Downstream flow through resulting from streamer incident at center of screen.

Figure 9e. Wake resulting from streamer incident near top of screen, showing low-frequency turbulence.

Figure 9f. Two examples of pulsed annuli on leeward (left-hand) side.

about 2.4 m/sec to about 1.4 m/sec. It was not possible to photograph the behavior inside the inner foam ball, but flow around it was smooth. On the leeward side of the screen, the wake and flow-through portions of the flow were clearly distinguishable. Wake turbulence was indeed at low frequencies, but it was kept well away from the screen by the smooth currents of emerging flow-through. Flow velocities just behind the screen were on the order of 0.5 m/sec, but they were seen to speed up farther away as wake effects became appreciable.

Pragmatically, this screen had several advantages. The plywood plates on the top and bottom provided structural strength to the windscreen and good weather protection for the microphones. However, a subsequent design eliminates both plates as possibly undesirable acoustically, and replaces them with a foam-covered skeleton. In 4 weeks of continuous exposure in the desert during field tests (described below), the foam showed no signs of deterioration. It is known, however, that polyurethane foam will become brittle under prolonged exposure to ultraviolet light–a lifetime of 1 year might be projected for continuous outdoor use. It has been found that in snowy conditions, the foam tends to collect ice in its pores, seriously impeding its flow-through characteristics. This problem might be overcome with a simple resistive heater if the screen were to be used in hard winter environ-

ments. The foam was attached to the frame using Velcro so it was readily removable. This allowed easy manipulation of the microphones and screening layers inside the screen. One further feature was that the microphones were mounted to allow adjustment of their vertical spacing.

Based on the three major problems it was designed to overcome, this screen was designated as an "Omnidirectional, Low-frequency, Outdoor microphone Windscreen" or "OLOW." The original wire screen was also tested in the field, and is shown in Figure 10. Its dimensions were similar to the OLOW, though slightly narrower and slightly taller. It employed three layers of wire mesh and provided a good basis for comparison of wire and foam screens.

Testing the Microphone Array for Its Ability To Reduce Wind Noise

The validity of the cross-product scheme depends on two points: wind noise must be reduced and the acoustic signal measurements must not be degraded. Buck and Greene's method promises to eliminate wind noise completely, but this will be the case only for an average over infinite time with infinite microphone spacing, which cannot be realized in practice. Furthermore, the premise of acoustic signal correlation is based on several

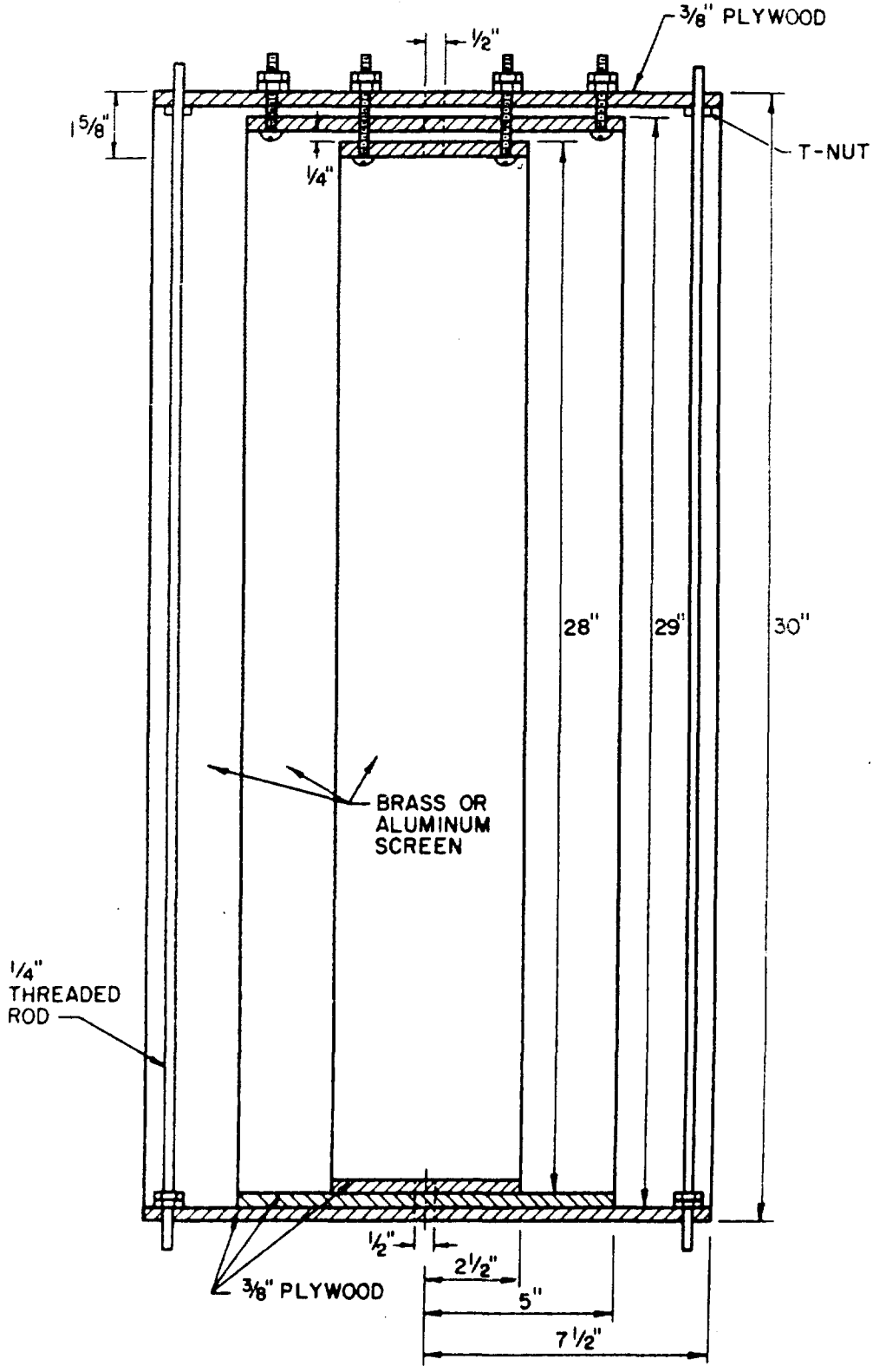

Figure 10. Original windscreen.

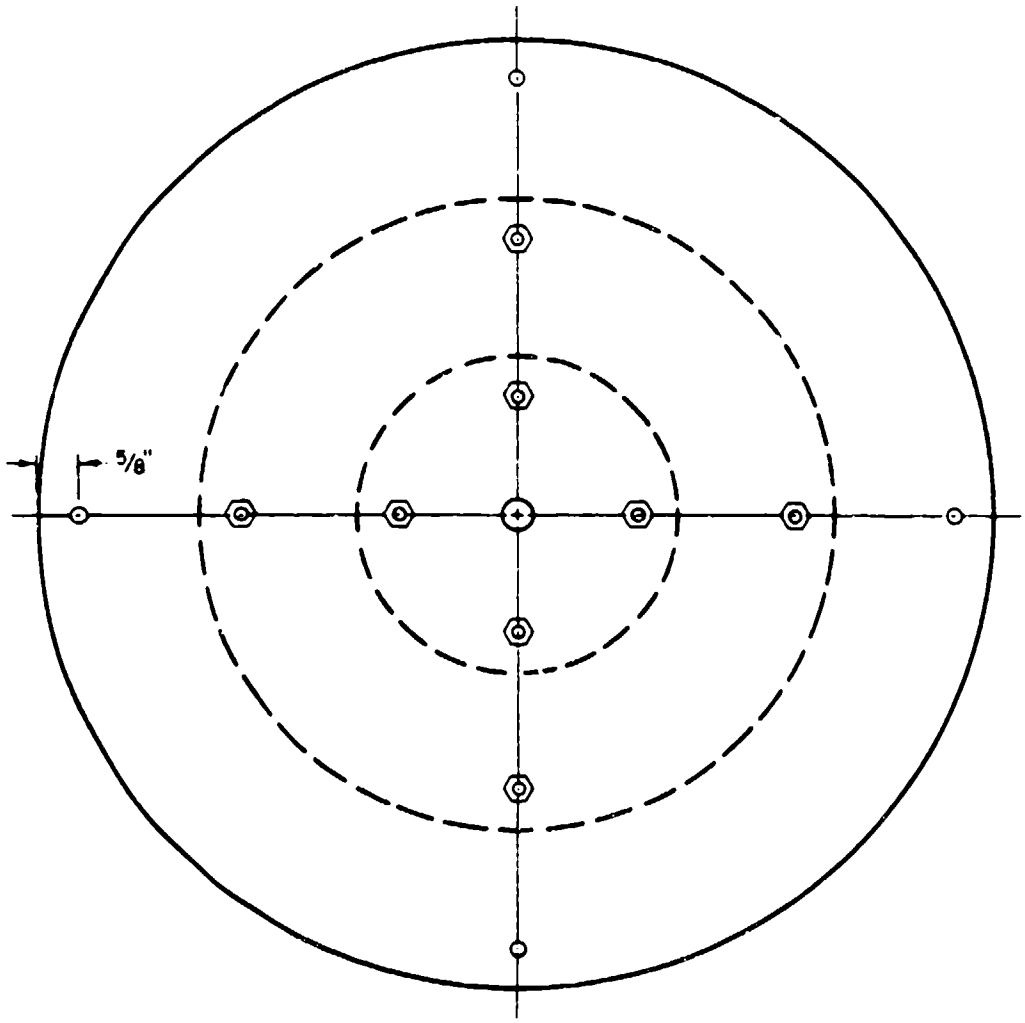

WINDSCREEN TOP VIEW

Figure 10. (Cont'd)

approximations and simplifications. Thus, both the achievable wind noise reduction and the degree of acoustic signal correlation must be determined empirically. These investigations are most easily done independently; that is, wind noise reduction is measured in the absence of significant acoustic signals, and acoustic signal (blast) correlation is examined in the absence of wind noise. However, ultimately, they are tested together.

A requirement common to all investigations is that the two microphones and their preamplifiers have nearly identical low-frequency phase response. The necessity of phase matching was made apparent by the early studies of blast peak coincidence, as described earlier. This requirement was met by using very low-frequency microphone systems and passing the outputs through a pair of closely matched, high-pass filters with a corner frequency well above that of the microphones.

The Measurement Index $\overline{\Delta L}$

In the following studies of the two-microphone system, the information sought is essentially how the system performs in comparison with a single microphone. To measure wind noise reduction, the output of a single microphone is needed to indicate how much wind noise was present to begin with; the noise level calculated by cross multiplying two outputs can be subtracted from this to find the noise reduction achieved. When correlated

acoustic signals are present, the one-microphone and cross-product levels should be the same, so that in this case the difference is inversely related to the degree of signal correlation. In both cases, the parameter of interest is the difference in measured sound levels, ΔL.

In practice, two microphone outputs are available; while both are required to find the cross-product sound level, either one can be used to find a single-microphone level. Thus, two versions of ΔL are possible:

$$\Delta L_1 = L_1 - L_X$$

and

$$\Delta L_2 = L_2 - L_X \tag{23}$$

from Equation (22), where L_X is the sound level found using the cross-product of two microphone signals and L_1 and L_2 are the single-microphone levels. It was decided to average these, since overall average values of ΔL were to be found anyway:

$$\begin{aligned} \overline{\Delta L} &= \frac{1}{2}(\Delta L_1 + \Delta L_2) \\ &= \frac{1}{2}(L_1 - L_X + L_2 - L_X) \\ &= \frac{1}{2}(L_1 + L_2) - L_X \qquad \text{dB} \end{aligned} \tag{24}$$

Thus the average ΔL for each measurement is the difference between the cross-product level and the average of the single-microphone levels.

This definition of ΔL turned out to have more significance than just as a convenience. The sound levels L_1, L_2, and L_X are defined in terms of the microphone pressure excitations $s_1(t)$ and $s_2(t)$; these, in turn, can be related to the microphone output voltages by $s(t) = gm(t)$, where $m(t)$ is the output voltage and g is the microphone gain in units of pascals (pressure) per volt. The level definitions are:

$$L_X = 10 \log[K \int_0^T s_1(t)s_2(t)dt] = 10 \log[K g_1 g_2 M_{12}] \quad (25)$$

$$L_i = 10 \log[K \int_0^T s^2(t)dt] = 10 \log[K g_i^2 M_{ii}] \quad \text{and } i = 1, 2 \quad (26)$$

with

$$M_{ij} = \int_0^T m_i(t)m_j(t)dt$$

where $K = 1/Tp_0^2$ for LEQ, or $1/t_0p_0^2$ for SEL. Substituting into the above definition for $\overline{\Delta L}$, we have

$$\begin{aligned} \overline{\Delta L} &= \frac{1}{2}(10 \log[K g_1^2 M_{11}] + 10 \log[K g_2^2 M_{22}]) - 10 \log[K g_1 g_2 M_{12}] \\ &= 10 \log[\sqrt{M_{11}M_{22}}/M_{12}] \quad \text{dB} \end{aligned} \quad (27)$$

The right-hand side of this equation is the absolute value of the normalized cross correlation of $m_1(t)$ and $m_2(t)$ at $t = 0$. This is important because many available measurement instruments, such as Bruel and Kjaer's 2032 Dual Channel Signal Analyzer or Data Precision's Data 6000, have the capability to calculate the normalized cross correlation as a function of time. Thus, the calculation of $\overline{\Delta L}$ required for the following investigations was possible without special data analysis equipment.

6 WIND NOISE REDUCTION INVESTIGATION

Procedure

The purpose of the wind noise reduction investigation was to measure the average wind noise reduction obtained by using the cross-product method to calculate the sound level. Wind noise samples were recorded in the absence of any significant acoustic signals; thus, the levels calculated represent wind noise error. Since $\overline{\Delta L}$ is the difference between the cross-product level and the average single-microphone level, it is equal to the wind noise reduction achieved for a given sample.

Two major parameters can be expected to affect the wind noise reduction. One is the sample length (the measurement period). As mentioned earlier, complete wind noise elimination can be obtained only by averaging over all time. Since blasts have a duration of up to about 1 second at far distances, 1 second wind samples were taken. If the wind noise process is assumed to be wide-sense stationary, these samples can be concatenated to study the effect of longer sample lengths.

The other parameter is the vertical spacing between the two microphones. The cross correlation between wind noise signals should in general decrease as the two microphones are moved farther apart. Daigle *et al.* have

found the typical correlation length of wind turbulence to be about 1.1 m near the surface of the earth [Ref. 34], so average wind noise reduction can be expected to approach a maximum for microphone spacing at or above this value. But the acoustic signal correlation might be reduced by increasing spacing, as suggested in Figure 7, so a trade-off may be required. Data were collected with microphone spacings of 30, 70, 90 and 110 cm; this represents the practical range of spacing.

The wind data were taken at the USACERL in Champaign, IL, on a flat rooftop about three stories off the ground. The rooftop measured 25 m by 37 m, and the microphone array was 5.4 m from the nearest edge and 19 m from the edge in the direction of prevailing winds. The surroundings consisted of low buildings and fields of grass and corn stubble. The experiment ran from February through April, 1984; average windspeeds ranged form 3.1 to 10.7 m/s, with peak gusts from 5.8 to 17.0 m/s. Fairly high winds were required due to the dynamic range of the microphones used (100 to 190 dB, SPL). Obviously, the data collected in this environment cannot be expected to represent every situation; no universal environment exists. Rather, these data serve as an indication of the results that can be expected for a highly turbulent flow, which is the worst case situation.

The microphones were positioned vertically, as in Figure 7, with the bottom microphone 167 cm from the rooftop. The upper microphone height was adjusted to vary the spacing. Ground effects on wind turbulence should be relatively small above 1 m, as found by Daigle *et al.* [Ref. 34], so the same average turbulence was expected at both microphones (overall average wind noise levels at the two microphones were very nearly equal, which verifies this assumption). The microphones used were piezoresistive (Endevco Model 8550M1), with preamplifiers and line drivers. The microphone systems had low frequency corners of $\sim$ 0.05 Hz. The signals were passed through a pair of single-pole high pass filters with $f_0 = 1.872$ Hz, matched to within 0.0168 degree of phase at f_0, so that the time shift between channels at f_0 was only 25 μs. Finally, the two signals were sampled at $f_S = 2$ kHz by a Norland 2001A digital calculating oscilloscope, which did most of the processing necessary to find the single channel and cross-product levels. Since wind noise has little or no significant energy above 1 kHz, aliasing was not a problem. Thirty-seven 1-second samples were taken with the microphones spaced 31 cm apart; 207 samples were taken at 70 cm, 108 samples were taken at 92 cm, and 114 samples were taken at 110 cm.

Results

The processed data for each microphone spacing are shown in Table 5. Results for sample lengths longer than 1 second were found by concatenating 1 second samples; as mentioned earlier, this procedure is valid if the noise is assumed to be wide-sense stationary. Thus, the number of samples available for a given sample length is equal to the number of 1 second samples in the original dataset divided by the sample length. The wind-induced noise level varied from 105 to 130 dB, with an overall average of 118 dB. No dependence of $\overline{\Delta L}$ on noise level was observed over this range. The average noise level was about the same for all spacings and sample lengths.

The observed distribution of the noise reduction factor $\overline{\Delta L}$ was approximately Gaussian, but with a rather large standard deviation. This indicates a wide fluctuation in the noise reduction achieved from sample to sample.

Figure 11 is a comparison of the wind noise reduction results, showing the dependence on spacing. The 31 cm data are always lowest, but the data for the other microphone spacings show no clear order; this indicates that the wind noise signal correlation changes very little for spacings between 70 and 110 cm. The wind noise reduction $\overline{\Delta L}$ depends inversely on wind noise correlation, so this indicates little increase in $\overline{\Delta L}$ over this range of microphone spacings. The wind noise reduction for wider spacings starts at

about 10 dB for a 1 second sample length and shows a gradual improvement of 3 to 4 dB as the sample length increases.

Table 5

Wind Noise Data: Normalized Cross Correlation $\overline{\Delta L}$

Microphone Spacing:	31 cm		70 cm		92 cm		110 cm	
Sample length ×1.024 sec	Mean (dB)	Std. Dev.	Mean (dB)	Std. Dev.	Mean (dB)	Std. Dev.	Mean (dB)	Std. Dev.
1	8.77	6.03	10.08	4.93	8.71	3.59	10.59	4.82
2	9.30	4.59	10.98	4.00	10.67	4.26	12.39	5.19
3	10.56	6.37	12.94	6.28	11.01	4.00	12.65	3.87
4	10.00	4.10	13.47	6.23	11.18	4.83	13.77	5.38
5	8.98	2.67	12.14	4.03	11.79	3.74	13.85	4.28
6	9.09	3.33	13.04	4.36	12.13	4.47	13.19	3.05
7	9.33	2.85	13.10	4.22	11.89	2.97	14.80	5.19
8			13.08	3.93	16.56	8.84	13.42	2.64
9			12.71	3.11	13.41	2.83	15.37	4.94
10			12.91	3.57	16.82	6.64	15.00	5.66
11			12.67	2.96	14.05	4.36	15.49	5.66
12			13.39	3.00	16.88	7.28	13.91	2.65
13			13.96	4.33	14.67	3.00	13.74	2.90
14			13.45	3.52	13.79	2.07	14.28	3.57
15			14.51	4.77	16.36	5.38	15.27	5.78
16			13.59	3.52	14.92	3.29	13.84	1.90
17			14.90	6.12	15.12	3.13	12.98	1.25
18			14.50	5.85	16.94	3.92	14.32	2.77
19			14.32	5.49	17.37	4.36	13.64	1.75
20			12.89	1.32	19.19	8.90	15.27	5.12

The 31 cm dataset consisted of 37 one second samples; at 70 cm there were 207 samples; at 92 cm, 108 samples; and at 110 cm, 114 samples.

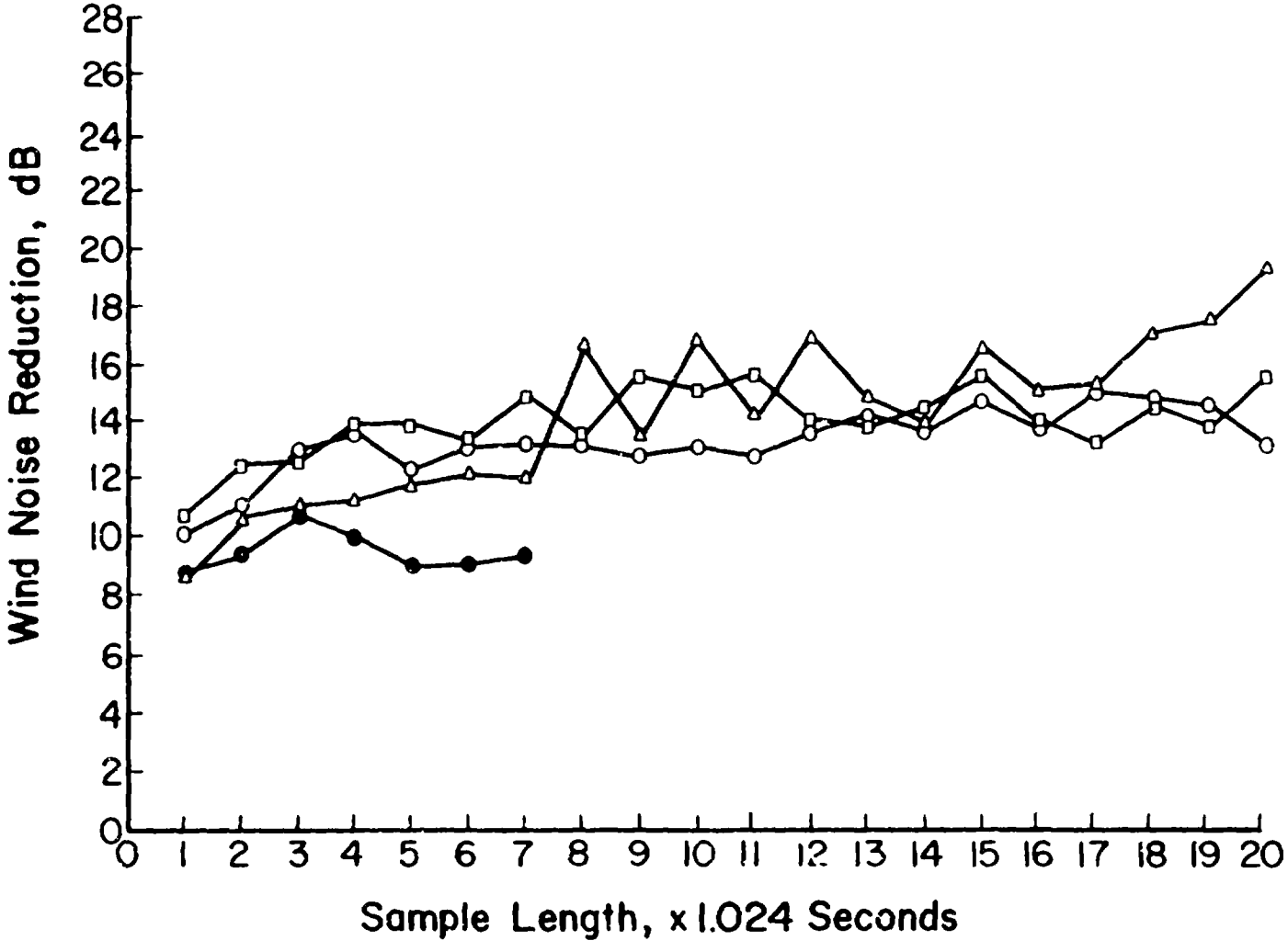

Figure 11. Comparison of wind noise reduction results.

Some additional data were taken with C-weighting filters to see if any further improvement in noise reduction would result. The C-weighting filter characteristic emphasizes those frequencies that shake buildings and cause objects to rattle. Thus, C-weighting is often used in blast noise sound level measurements to give an accurate indication of the annoyance level due to a given blast [Ref. 35, 36]. C-weighting attenuates most of the signal energy below 20 Hz [Ref. 37], so that C-weighted wind noise signals will have shorter average wavelengths and should be less correlated than flat-weighted signals for a given microphone separation.

Unweighted and C-weighted data were collected in August and September of 1984. The microphone separation was 110 cm; the results are shown in Table 6.

The results for the flat-weighted samples agree with those for the 110 cm microphone separation data collected the previous spring. But the C-weighted samples have an average noise reduction almost twice as high, with a relatively small increase in the standard deviation. Thus, where C-weighting can be used, a significant improvement in wind noise reduction may be achieved.

Table 6

Wind Noise Data: Effect of C-Weighting

Filtering	Sample Length	No. of Samples	$\overline{\Delta L}$ (dB)	Std. Dev. of $\overline{\Delta L}$ (dB)
Flat-weighted (2 Hz matched high pass filter only)	1 sec	154	11.5	5.0
C-weighted (matched pair: phase difference of 0.0239° at 10.0 Hz)	1 sec	150	21.7	6.2

7 TESTING THE COMBINED METHODS WITH BLASTS IN WIND

Sites for Data Collection

This chapter describes the final tests, in which the improved windscreens were combined with the two-microphone array and which were conducted with real blast sound in the presence of wind. Two sites were used to collect data for the experiment. The first site was Fort Sill, OK, where 6 weeks were spent collecting data in July and August 1986. The second site was Fort Leonard Wood, MO, where 2 weeks were spent collecting data in January 1987. These two sites were chosen because of their flat open topography, and because the necessary blast sounds could be generated and measured several times a day. Moreover, according to weather data, these two sites had a high probability of strong wind conditions at the respective times of year for these measurements.

Fort Sill is an artillery training school with many different sites for firing. The landscape is relatively flat grassland, with occasional shallow ponds. The weapons used to generate blast sounds were 105 mm and 155 mm Howitzers. Since the artillery fired at different sites each day, the measurement site moved each day.

At both sites, a 5-ton truck served as the mobile acoustics lab, holding all the equipment. At Fort Sill, its generator supplied all the power necessary to perform the measurements.

There were many blasts per day to measure at Fort Sill, but the wind conditions were fairly light. Out of the 6 weeks spent there, the wind reached 44 m/s (20 mph) on only 2 days, and a mild 22 to 33 m/s (10 to 15 mph) on 2 other days. The rest of the time, there was no significant wind.

Fort Leonard Wood's landscape consists of rolling wooded hills with a few barren, rocky areas. There were two blast sites, one 5.7 km to the east, and the other 10.4 km to the west of the microphones. The blast sound was generated with $1\frac{1}{4}$-lb and 5-lb charges of C-4 (plastic explosives). In these tests, the two blast sites and the measurement site were stationary. Wind conditions were good and many data were collected under high wind velocities.

Procedure

The equipment used to acquire data is shown in Figure 12. A Precision Data 6000 was added to aid with checking and analysis of the data. The equipment was calibrated every day before data were collected using a piston phone (B & K type 4220). For each microphone, this calibration signal was

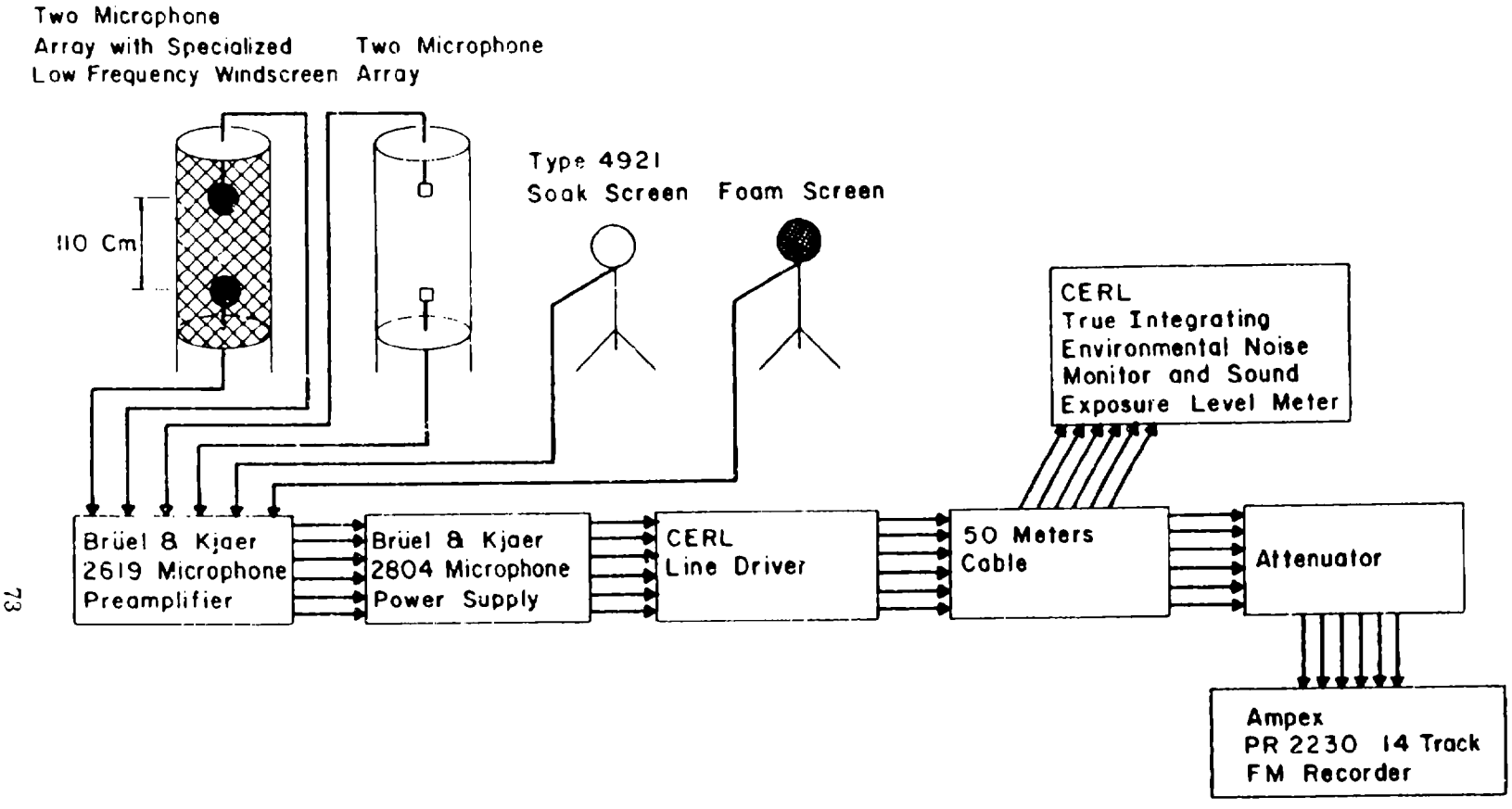

Analysis of Data

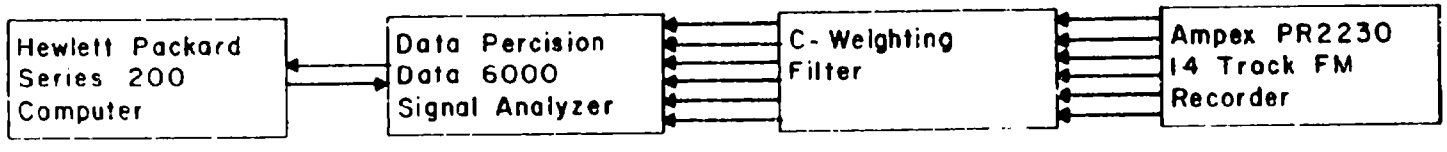

Figure 12. Data acquisition equipment.

recorded on an Ampex PR 2230 FM type recorder for a period of no less than 1 minute and checked using the Precision Data 6000.

The setup of the microphones was slightly different at the two locations. At Fort Sill, five microphones were used: one bare microphone, one with a 19 cm foam ball windscreen, one with a 12 cm nylon mesh ball-shaped windscreen, and two inside the special low-frequency windscreen (OLOW). Six microphones were used at Fort Leonard Wood. Instead of having a single, bare microphone, two microphones were used in a vertical array, as they would be inside the special low-frequency windscreen, but without the windscreen. The rest of the microphones were set up the same as at Fort Sill. Figure 13 shows the microphone setup at Fort Leonard Wood. To prevent any systematic biases to the data, the windscreens and their materials were rotated among the microphone positions. The USACERL True Integrating Noise Monitor [Ref. 32], an instrument to measure SEL, was used on-line to determine blast levels. These measured SELs were used later as a check during processing of the data.

The FM recorded tapes were played back through matched C-weighted filters as a part of the analysis. A Hewlett Packard computer was used to control the "capture" of blast signals by the Precision Data 6000 and its calculation of SEL, LEQ, cross product, and absolute value of the cross

Figure 13. Microphone setup at Fort Leonard Wood.

product. These statistics were calculated every 1/10 of a second, for 10 and 30 second periods. (The Fort Sill data are recorded on 10-second sections of tape and the Fort Leonard Wood data are recorded on 30-second sections of tape.)

8 RESULTS

Windscreen Transparency

Examination of the data from this phase of the study showed that all the windscreens used in this experiment are acoustically transparent; that is, they do not change the magnitude or phase of the incoming signal. Moreover, the windscreen is acoustically transparent in the presence of wind; there are no interactions between transparency and the presence or absence of wind. Several blasts were measured during windy conditions and all the different windscreen-microphone setups measured the same SEL and peak levels, so long as the signals were not buried in wind.

Blast Detection Using a Two-Microphone Array

To show the effectiveness of the two-microphone array, data with peak blast levels approximately equal to wind noise levels were observed. Four plots of the processed data are shown in Figures 14 through 17. The first three plots are for the bare, two-microphone array. The last plot is for the two-microphone, special low-frequency windscreen array. Two of the plots are examples of blasts with peak levels close to the level of the background wind noise level. The third plot (Figure 16) shows the ineffectiveness of the two-microphone array when the blast level is below the wind noise level.

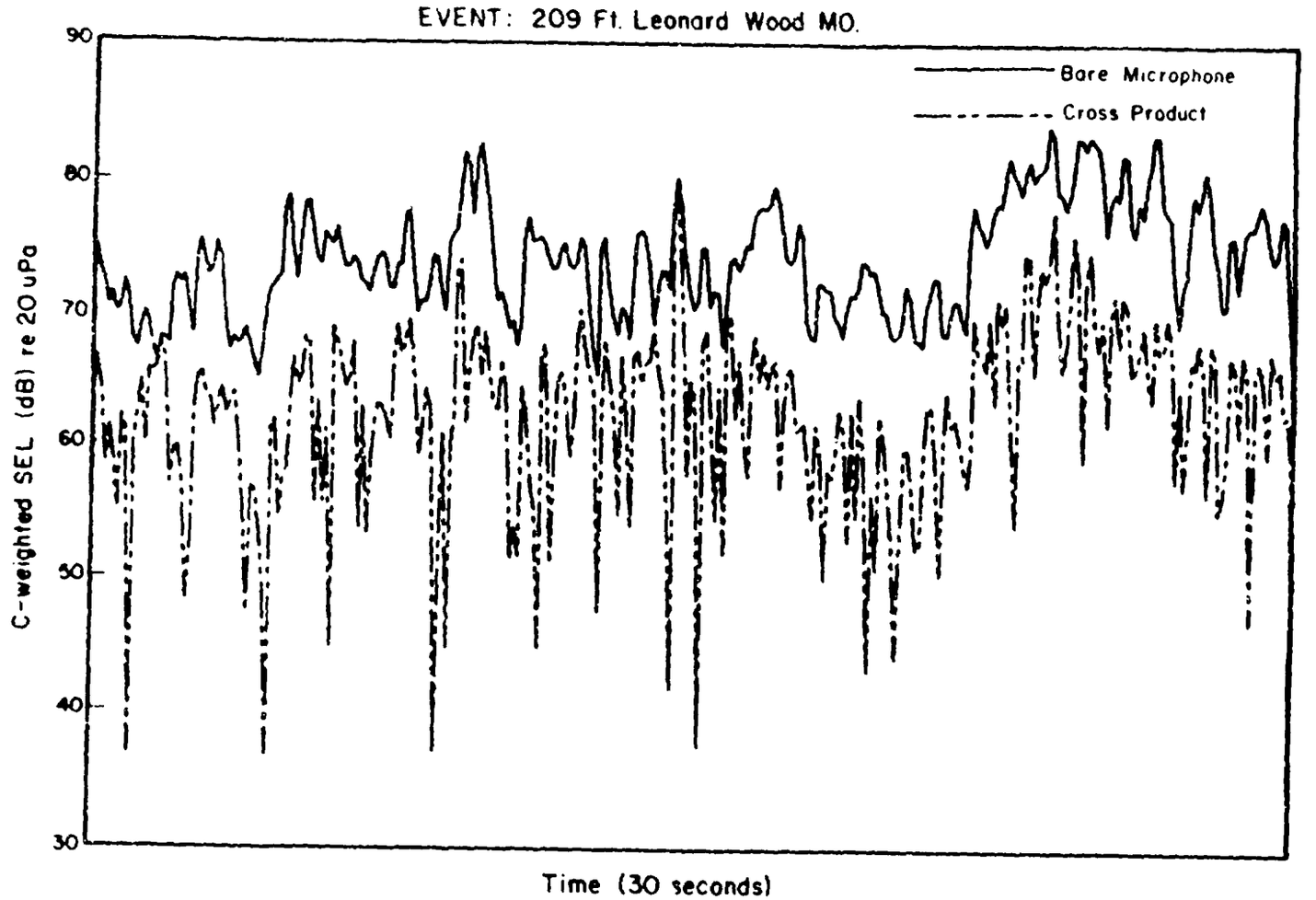

Figure 14. Processed data plot, Event 209, using bare, two-microphone array.

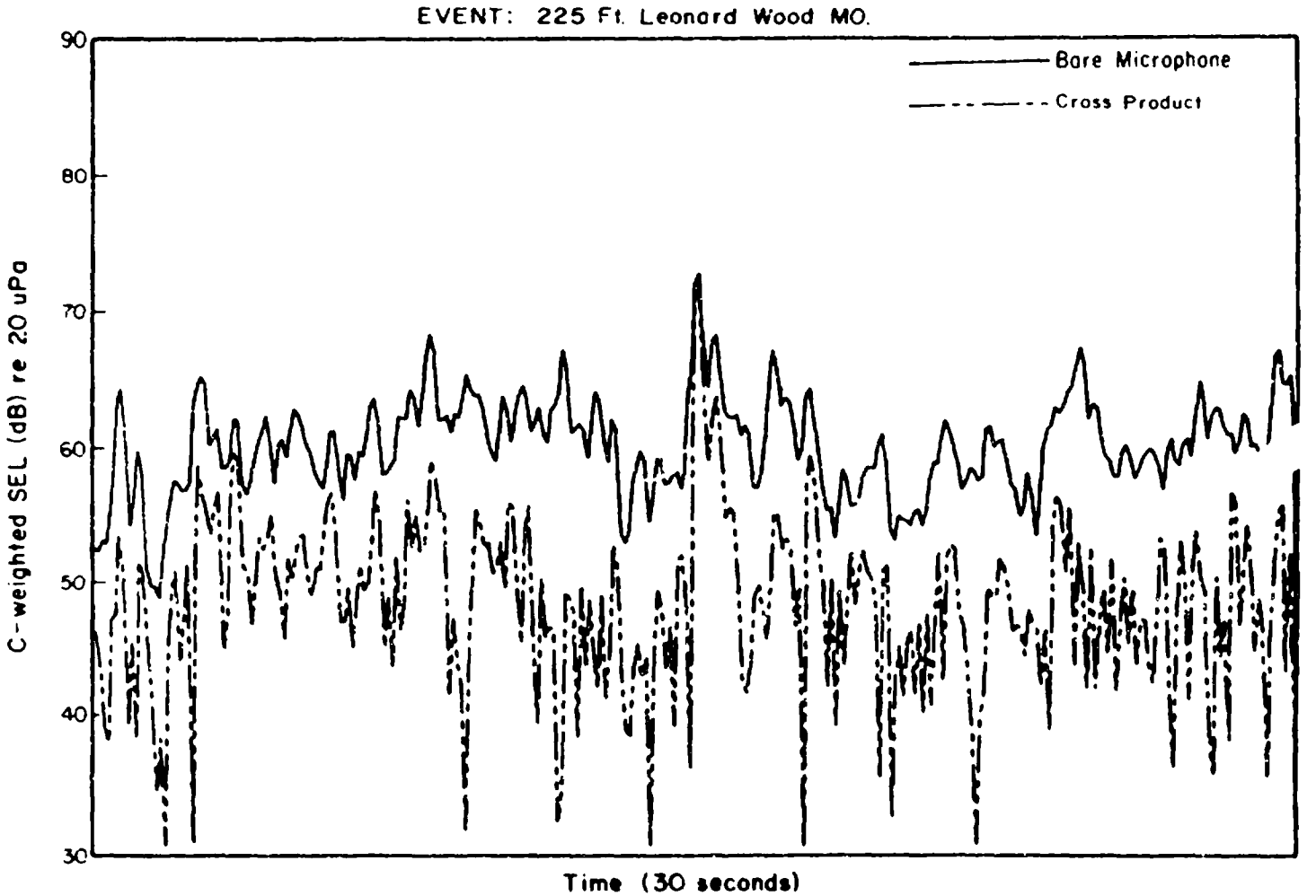

Figure 15. Processed data plot, Event 225, using bare, two-microphone array.

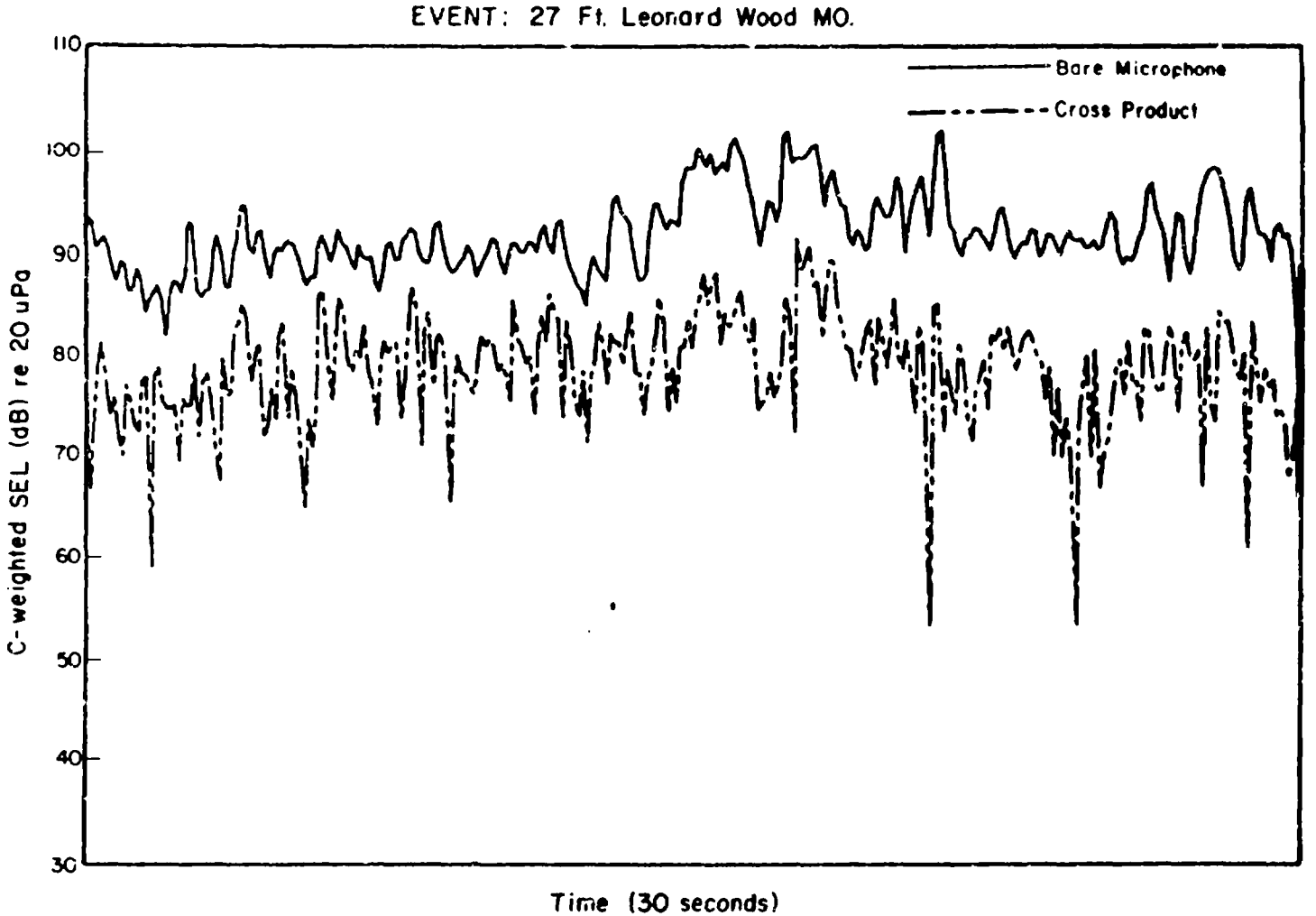

Figure 16. Processed data plot, Event 27, using bare, two-microphone array.

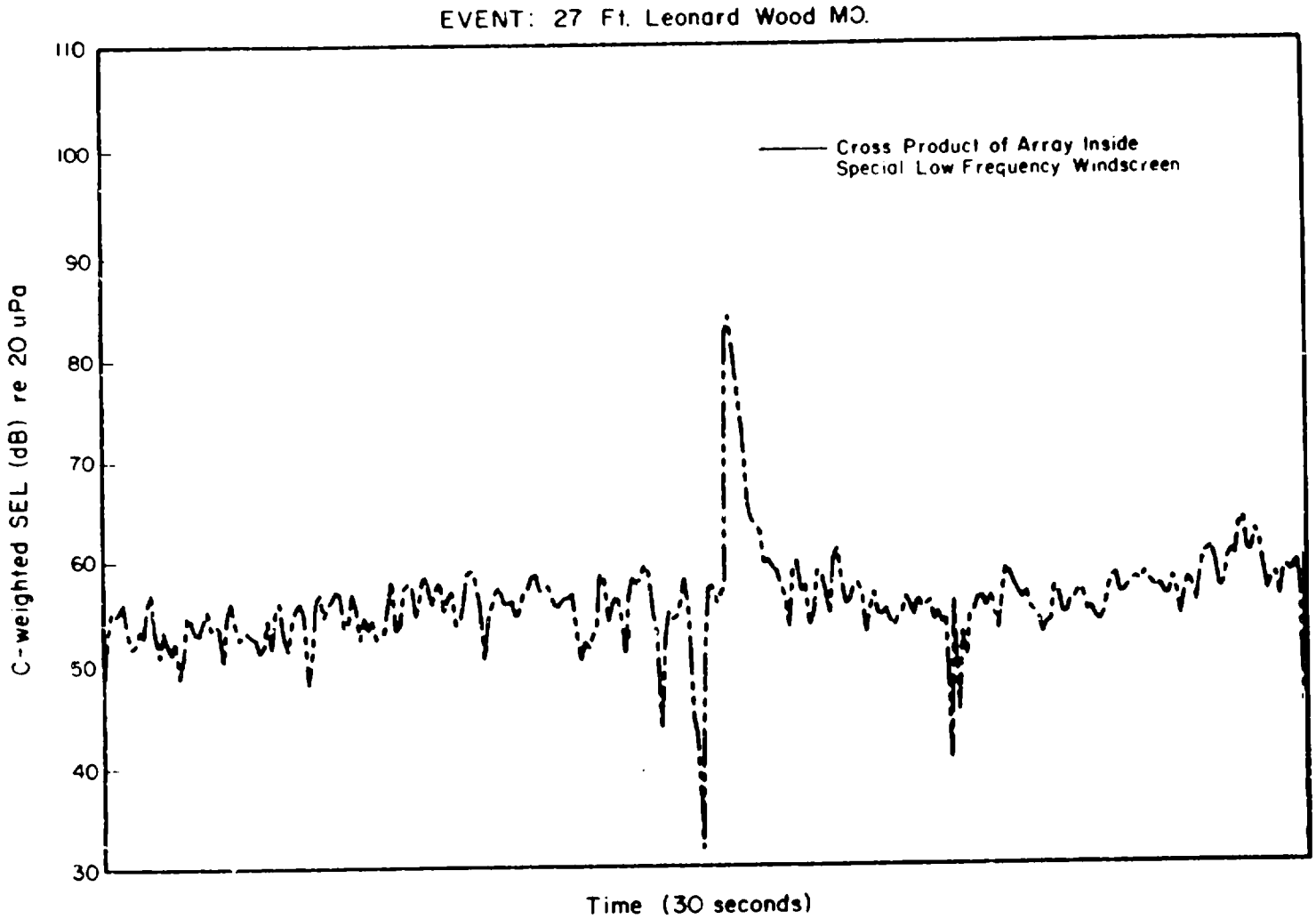

Figure 17. Processed data plot, Event 27, using low-frequency windscreen array.

These data were recorded on two different days at Fort Leonard Wood. The data plotted in Figure 14 were recorded during a period of 6.2 m/sec winds, the data plotted in Figure 15 were recorded during a period of 5.2 m/sec winds, and the data in Figure 16 were recorded during 10.3 m/sec winds. In each plot the time axis is 30 seconds long. Each plot includes one blast signal which lasts for approximately 0.5 second during 30 seconds of background wind data. The vertical axis is a measure of 0.2 second SEL in dB ($re\ 20\ \mu Pa$). The signals were first C-weighted, and Eq. 16 was used to calculate SEL for the "louder" of the two, single microphones, and $p^2 = p_1 p_2$ was used to calculate the integrated cross product for the two-microphone case. The cross product was taken between two vertically placed, bare microphones separated by 110 cm. The integration period in the figures displayed is 0.2 second but the integral was actually calculated every 0.1 second, so for each curve, this 0.1 second SEL was calculated 300 times.

The plots in Figures 14 and 15 show the blasts occurring close to the center of the measurement time period. In each of these two plots, the blast signal can be identified by observing the large peak in the cross-product curve approaching a peak in the single microphone curve. In these two plots, it is clearly impossible to detect the blast using a threshold with a

single, unscreened microphone. But the integrated cross-product curves in both figures show that a a detection algorithm could be developed which would make use of the fact that the integrated cross-product approached the single microphone signal only when the correlated blast was present. With no windscreen, blasts having a C-weighted SEL below 80 dB could be detected. The improvement is dramatic.

The third plot, Figure 16, is a case where the wind noise was about 10 dB greater than the level of the blast. The blast SEL was 82 dB. In this case, it is impossible to distinguish where the blast occurred in the integrated cross-product curve. But Figure 17, portraying the same time period as Figure 16, shows the integrated cross product of signals from two microphones using the specialized low-frequency windscreen (OLOW). Here, the blast is clearly distinguishable.

Overall Wind Noise Reduction

The background wind noise was examined for each event, and an LEQ was found for each microphone. Equation 17 was used to find LEQ for each of these cases: (1) the single microphone case, (2) the integrated cross-product case, and (3) the absolute values of the factors in the integrated cross-product case. This third case, the absolute values of the factors, was

included as a lower bound on the applicability of the integrated cross product method. The integration period to calculate the LEQ for each event was 15 seconds. The results are listed in Table 7.

An overall average wind noise reduction was calculated for each type of windscreen. The average wind noise reduction was calculated by summing the separate trial LEQs for each individual type of windscreen and then dividing by the number summed. The results show the average C-weighted wind noise reduction for each type of windscreen to be: 9.2 dB for the absolute values of the factors in the integrated cross product of two bare microphones, 22.2 dB for the integrated cross product of two bare microphones, 19.3 dB for the 12 cm nylon mesh covered wire frame ball windscreen, 23.6 dB for the 17 cm diameter solid foam ball windscreen, about 29.5 dB for the either microphone inside the specialized low-frequency windscreen, and 32.2 dB for both the integrated cross product and the absolute values of the factors is the integrated cross product for the two microphones inside the specialized low-frequency windscreen.

At first glance, these results apparently indicate only a 3.0 dB improvement in wind noise reduction when comparing the integrated cross product of the two-microphone array inside the low-frequency windscreen with the level measured by one microphone inside the same windscreen. On the other

Table 7

C-Weighted Wind Noise Reduction (dB)

(1)	(2)	(3)	(4)	(5)	(6)	(7)	(8)	(9)
006	11.2	-12.2	-20.2	-24.3	-30.2	-30.2	-30.6	-31.3
007	9.15	-7.7	-15.1	-17.7	-19.0	-19.5	-19.7	-20.5
008	9.19	-6.8	-29.1	-18.2	-19.9	-20.4	-20.8	-21.7
009	9.60	-7.6	-24.3	-18.5	-22.6	-25.8	-26.5	-29.2
026	10.3	-10.8	——	——	——	-37.9	-37.7	-43.0
027	10.3	-10.6	——	——	——	-32.5	-32.4	-35.7
209	6.02	-8.24	——	——	——	-27.9	-28.6	-30.1
159	4.5	——	——	-19.4	-24.6	-31.5	-30.0	-34.4
171	4.9	——	——	-23.5	-23.1	-33.2	-30.8	-37.4
191	3.7	——	——	-19.7	-23.6	-32.1	-29.5	-35.2
190	4.2	——	——	-16.3	-26.6	-32.5	-31.6	-33.4
192	5.0	——	——	-16.3	-22.3	-32.1	-32.0	-34.8
				Average Values				
		-9.2	-22.2	-19.3	-23.6	-29.6	-29.2	-32.2

(1) Event number
(2) Windspeed (m/sec)
(3) Absolute value of the cross product of bare microphone array
(4) Cross product of bare microphone array
(5) Nylon ball windscreen
(6) Solid foam ball windscreen
(7) Bottom microphone inside low-frequency windscreen
(8) Top microphone inside low-frequency windscreen
(9) Both cross product and abolute value of the cross product for the microphone array inside the low-frequency windscreen.

hand, taking the integrated cross product of the two bare microphones shows an improvement of 22.2 dB over the level of a single bare microphone.

There are at least three explanations for this unexpected result: (1) the dynamic range of the Ampex PR 2230 tape recorder is limiting the results, (2) the ambient acoustical background noise is limiting the results, or (3) the windscreen is somehow reacting with the wind and causing the signals measured at each microphone to be correlated. Tests were performed as described below and it was determined that the small improvement in wind noise reduction was due to the background acoustical noise and the noise floor of the tape recorder. These both limit the ability of the integrated cross-product method to reduce the wind noise any further than is already accomplished by the windscreen alone.

The data collected at Fort Leonard Wood showed little improvement when taking the integrated cross product of the two microphones inside the special low-frequency windscreen because of the background noise. About 1/2 to 1 mile away from the microphones were about 25 to 50 large pieces of tracked, earth-moving equipment such as bulldozers, scrapers, and graders. This equipment generated low-frequency noise which was received by the microphones. Basically, for speeds less than about 25 mph, the windscreen reduced most of the wind noise. Therefore, the microphones were measuring

background noises since the windspeeds never exceeded 55 m/s (25 mph). This background C-weighted noise level varied from 55 to 65 dB, and it obviously was correlated at each of the two microphones. Therefore, taking the integrated cross product of two correlated signals yielded no improvement.

In contrast, nearly all the time at Fort Sill, the background C-weighted noise level was much lower. Some of the analyzed Fort Sill data, such as those shown in Figure 18, showed large cancellations when taking the integrated cross product of the two microphones inside the special low-frequency windscreen. This figure suggests that the background noise recorded at Fort Sill was limited by the noise floor of the tape recorder. Thus, in this case, the improvement realized by taking the integrated cross product was a reduction in the electrical noise of the tape recorder and not a reduction in wind noise. However, it is still a reduction in noise and generally indicates the applicability of the integrated cross product technique for separating signal from noise.

In summary, the integrated cross product method accomplishes 22 dB of wind noise reduction when the unscreened, two microphone array is used. However, when the background acoustical ambient approaches the level to which a highly efficient windscreen reduces wind noise, very little additional wind noise reduction can be accomplished. There is no evidence to suggest

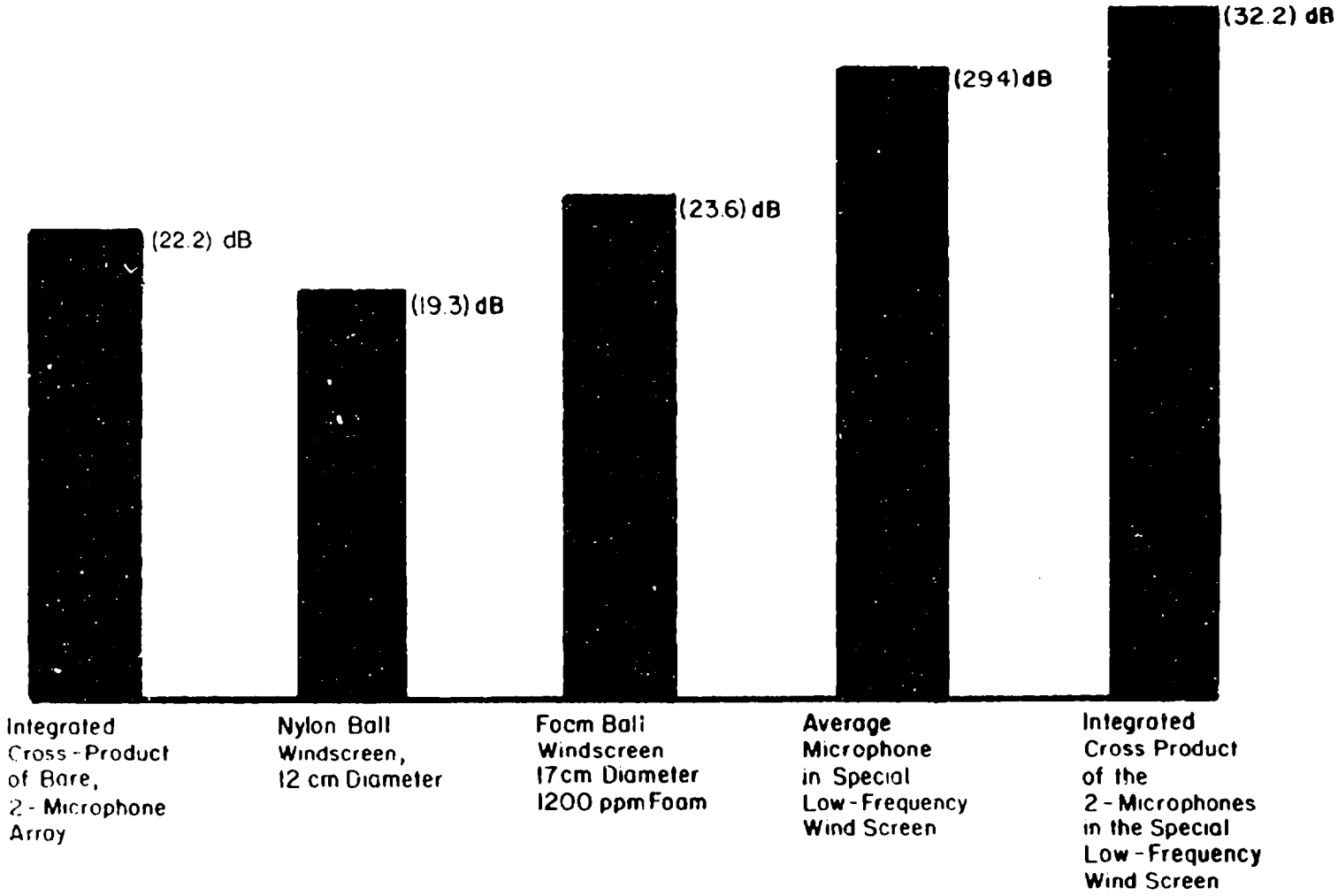

Figure 18. Overall C-weight noise reduction in dB (15 second LEQ) compared to a bare microphone.

that the windscreen design is somehow interacting with the wind to generate a separate correlated signal at the two microphones. So the two methods—the highly efficient windscreen and the integrated cross-product—can be used together effectively only when the winds are very high or the acoustical ambient is very low. Otherwise, together they are too good and limited by the acoustical ambient.

9 CONCLUSIONS

The windscreens used in the experiment are all acoustically transparent. The different windscreens reduced the background wind noise by differing amounts. For blast noise, the windscreen that is most economical and simplest to use while still yielding a fair degree of wind noise reduction is the 19 cm foam ball. If required for more critical situations, the specialized low-frequency windscreen can add 6 dB in C-weighted wind noise reduction.

Since the special low-frequency windscreen is layered and works so well, a layered windscreen could possibly be developed and used with a single microphone. It could be possible to achieve 29 dB of C-weighted wind noise reduction with a simple setup and processing system.

The cross product of two vertically spaced microphones can yield very significant wind noise reduction. With bare microphones, this technique yields 22.2 dB (C-weighted) which is in good agreement with the earlier results of 21.7 dB found on the roof of the laboratory. Taking the absolute values of the factors in the integrated cross product yields 9.2 dB.

The integrated cross-product method with the special low-frequency windscreen yields 32.2 dB of C-weighted wind noise reduction. This is only a 3 dB improvement in wind noise reduction over a single microphone inside the body of the special low-frequency windscreen. This small improvement in wind noise reduction is due to the windscreen reducing

most of the wind noise and the two microphones measuring only the residual correlated background noise. If the windspeeds were greater than 55 m/s (25 mph), then it might be possible to gain 20 dB or so in wind noise reduction. By using the special low-frequency windscreen and taking the integrated cross product, it might be possible to gain up to 50 dB of wind noise reduction. To accomplish this, the wind would have to be blowing at very high speeds or the background acoustical ambient would have to be very low, and the overall analysis system used would have to have an excellent dynamic range.

REFERENCES

1. Schomer, P.D., R.J. Goff, and L.M. Little, *The Statistics of Amplitude and Spectrum of Blasts Propagated in the Atmosphere*, Technical Report N-13/ADA033475, Vol 1, (U.S. Army Construction Engineering Research Laboratory [USACERL], November 1976).

2. Phelps, W., *Microphone Wind Screening*, RCA Review 3 (1938), pp 203-212.

3. Rasmussen, G., "Windscreening of Microphone," unpublished (A/S Burel and Kjaer).

4. Oswald, L.J., "The Wind Noise of Nose-Cover Protected Microphones," Proceedings of Inter-Noise 76 (Washington, DC, April 5-7, 1976), pp 141-144.

5. Nakamura, A., R. Matsumoto, A. Suginuma, and T. Tanaka, "Some Investigations on Output Level of Microphones in Air Streams," J. Acoustical Soc. Am., Vol 46, No. 6 (December 1969), pp 1391-6.

6. Neise, W., "Theoretical and Experimental Investigations of Microphone Probes for Sound Measurements in Turbulent Flow," *J. Sound and Vibration*, Vol 39, No. 3 (April 8, 1975), pp 371-400.

7. Bleazy, J.C., "Experimental Determination of the Effectiveness of Microphone Wind Screens," *J. Acoustical Soc. Am.*, Vol 9, No. 1 (January 1969), pp 48-53.

8. Bauer, B.B., "Design and Measurement of Infrasonic Gradient Microphones and Windscreens," *J. Acoustical Soc. Am.*, Vol 44 (November 1968), pp 1428-36.

9. M. Strasberg, "Dimensional Analysis of Windscreen Noise," *J. Acoustical Soc. Am.*, Vol 83 (February 1988), pp 544-48.

10. Thorne: U.S. Patent No. 588,034, August, 1897.

11. Spotts: U.S. Patent No. 1,901,065, August, 1933.

12. Beranek, L., *Acoustics* (McGraw-Hill, 1954), pp 133-134.

13. *Urethane Foams for Flexibility in Air Filtration Systems: Plastics Design and Processing* (Lake Publishing Corp., February 1979).

14. Davenport, A.G., "The Dependence of Wind Loads on Meteorological Parameters," *Wind Effects on Buildings and Structures*, Proceedings of the International Conference, Ottawa, Canada, Vol 1 (University of Toronto Press, 1967), p 37.

15. Duchene and Marullaz, *Wind Effects on Buildings and Structures*, Proceedings of the 4th International Wind Conference, Toronto, Canada (University of Toronto Press, 1975), pp 26-29.

16. Reynolds, A., *Turbulent Flows in Engineering* (John Wiley and Sons, 1974), pp 10ff.

17. Achenbach, E., "The Effects of Surface Roughness and Tunnel Blockage on the Flow Past Spheres," *J. Fluid Mechanics*, Vol 65, No. 1 (January 1974), pp 113-125.

18. Hosier, R.N. and P.R. Donovan, "Microphone Windscreen Performance," National Bureau of Standards NBSIR 79-1599 (1979).

19. Hosier and Donovan, pp 7, 35, and 37.

20. Ballard, H.N., and M. Izquierdo, "Reduction of Microphone Wind Noise by the Generation of a Proper Turbulent Flow," U.S. Army Regulation AR262, DDC No. AD455966 (February 1965).

21. P.M. Morse and K.U. Ingard, *Theoretical Acoustics* (Princeton Univ. Press, Princton, NJ, 1986), pp 701-5.

22. Daigle, G.A., J.E. Piercy, and T. F. W. Embleton, "Effects of Atmospheric Turbulence on the Interface of Sound Waves Near a Hard Boundary," *J. Acoustical Soc. Am.*, Vol 64, No. 2 (February 1978), pp 624-628.

23. Wagner, M., "Wind Noise Reduction in Blast Noise Measurement," Master's Thesis, University of Illinois, Urbana-Champaign (May 1983).

24. Brown, J., and R. Rowlands, "Design of Directional Arrays," *J. Acoustical Soc. Am.*, Vol 31 (1959), pp 1638-1643.

25. Anderson, V., *Digital Array Phasing*, Proceedings of the 58th Meeting of the Acoustical Society of America (1959).

26. User, T., "Signal Detection by Arrays With Arbitrary Processors and Detectors," *J. of the Acoustical Soc. Am.*, Vol 39, No. 1 (January 1966), pp 79-86.

27. Remley, W., "Some Effects of Clipping in Array Processing," *J. Acoustical Soc. Am.*, Vol 39, No. 3 (March 1966), pp 702-707.

28. Edelblute, R.K., "Criteria for Optimum Signal-Detection Theory for Arrays," *J. Acoustical Soc. Am.*, Vol 41, No. 1 (January 1967), pp 199-205.

29. Buck, B., and C. Greene, "Two-Hydrophone Method of Eliminating the Effects of Nonacoustic Noise Interference in Measurements of Infrasonic Ambient Noise Levels," *J. Acoustical Soc. Am.*, Vol 65, No. 5 (May 1980), pp 1306-1308.

30. American National Standard Institute (ANSI) Standard S12.9-1988, *American National Standard Quantities and Procedures for Description and Measurement of Environmental Sounds, Part 1* (ANSI, 1988).

31. Schomer, P.D., A.J. Averbuch, and L.M. Lendrum, *An Army Blast Noise Warning and Monitoring System*, Technical Report N-88/03/ ADA191230 (USACERL, February 1988).

32. Data Precision Corporation, *Data 6000 Users Guide* (1984).

33. Van Klotzsch, P., "Zur Windgerauschdampfung von Windschermen," *Hochfrequenztechnik u. Elektroakustik*, Vol 80, No. 1 (Leipzig, January 1971), pp 1-9.

34. Daigle, G.A., J.E. Piercy, and T.F.W. Embleton, "Propagation of Noise Over Short Distances Above Asphalt-Refractive and Impedance Effects," *J. Acoustical Soc. Am.*, Vol 73, Supplement 1 (Spring 1983), p S58.

35. Schomer, P.D., and R.D. Neathammer, *Community Reaction to Impulsive Noise: A 10-Year Research Summary*, Technical Report N-167/ ADA141762 (USACERL, February 1984), p 185.

36. ANSI Standard S12.4-1986, *Method for Assessment of High-Energy Impulsive Sounds With Respect to Residential Communities* (ANSI, 1986).

37. ANSI Standard S1.4-1971, *Sound Level Meters* (ANSI, 1971).

APPENDIX:

NOISE TERM ANALYSIS

In analyzing sound level measures in the presence of nonacoustic noise, several noise error terms arise. These are random variables whose characteristics depend on the properties of the noise process. In this development, an approximate model for the noise process is used to derive expressions for the means and variances of the three types of noise error terms encountered, as functions of the sound level measurement period T. These statistics are useful in predicting the effectiveness of the two-microphone noise reduction method.

The noise process is approximated by the Gauss-Markov random process with zero mean and autocorrelation

$$R_n(t,s) = \sigma_n^2 \exp(-b|t-s|) \tag{A1}$$

where σ_n^2 is the noise variance and $1/b$ is the correlation time. Both the nosie and the acoustic pressure can be reasonable represented as having zero mean, since a coupling capacitor can be used to eliminate any voltage

offset in the microphone signal. The model for the autocorrelation is appropriate because its power spectrum, given by

$$S_n(f) = 2b\sigma_n^2/(b^2 + 4\pi^2 f^2) \quad , \tag{A2}$$

is very similar to typical wind turbulence spectra. In particular, $S_n(f) \propto f^{-2}$ for large f: This dependence closely approximates the $f^{-5/3}$ rule for wind turbulence spectra at high frequencies [Ref. 22], [Ref. 23]. This model allows closed form expressions to be found for most of the noise term statistics, and it is a close enough approximation so that the results of the analysis accurately represent the dependence of the noise term statistics on the measurement parameters.

The first noise term to be analyzed is $\int_0^T p(t)n(t)dt$. The mean of this expression is given by:

$$E\{\int_0^T p(t)n(t)dt\} = \int_0^T p(t)\,E\{n(t)\}dt = 0 \tag{A3}$$

since the noise mean is zero. Because the expectation operator is linear, one also has

$$E\{\frac{1}{T}\int_0^T p(t)n(t)dt\} = \frac{1}{T}(0) = 0 \tag{A4}$$

A general expression for the variance of a random variable is

$$\begin{aligned} \mathrm{Var}[X] &= E\{X^2\} - E^2\{X\} \qquad \text{(A5)} \\ \text{But } E\{\int_0^T p(t)n(t)dt\} &= 0, \text{ so} \\ \mathrm{Var}[\int_0^T p(t)n(t)dt] &= E\{[\int_0^T p(t)n(t)dt]^2\} \\ &= E\{\int_0^T p(t)n(t)dt \int_0^T p(s)n(s)ds\} \\ &= \int_0^T \int_0^T p(t)p(s)E\{n(t)n(s)\}\,dtds \\ &= \int_0^T \int_0^T p(t)p(s)R_n(t,s)dtds \qquad \text{(A6)} \end{aligned}$$

This cannot be evaluated without knowing the acoustic pressure $p(t)$. However, since $p(t)$ has zero mean and $R_n(t,s) > 0$ for all t and s, the variance can be expected to be fairly small, independent of T. With the factor of $1/T$, the variance is

$$\begin{aligned} \mathrm{Var}[\frac{1}{T}\int_0^T p(t)n(t)dt] &= E\{[\frac{1}{T}\int_0^T p(t)n(t)dt]^2\} \\ &= \frac{1}{T^2}E\{[\int_0^T p(t)n(t)dt]^2\} \\ &= \frac{1}{T^2}\int_0^T \int_0^T p(t)p(s)R_n(t,s)dtds \qquad \text{(A7)} \end{aligned}$$

This variance will again be small for any value of T; it vanishes completely as T goes to infinity.

The second type of noise term has the form $\int_0^T n^2(t)dt$. The mean is

$$E\{\int_0^T n^2(t)dt\} = \int_0^T E\{n^2(t)\}dt \tag{A8}$$

Now, $\sigma_n^2 = E\{n^2(t)\} - E^2\{n(t)\}$ from Equation (A.5), but the latter term is zero, so $\sigma_n^2 = E\{n^2(t)\}$ and one has

$$E\{\int_0^T n^2(t)dt\} = \int_0^T \sigma_n^2 dt = T\sigma_n^2 \tag{A9}$$

Thus, the mean is directly proportional to T. With averaging, the mean is

$$E\{\frac{1}{T}\int_0^T n^2(t)dt\} = \frac{1}{T}(T\sigma_n^2) = \sigma_n^2 \tag{A10}$$

To find the variance, one first finds $E\{|\int_0^T n^2(t)dt|^2\}$:

$$\begin{aligned} E\{|\int_0^T n^2(t)dt|^2\} &= E\{\int_0^T n^2(t)dt \int_0^T n^2(s)ds\} \\ &= \int_0^T \int_0^T \Gamma\left\{n^2(t)n^2(s)\right\} dtds \end{aligned} \tag{A11}$$

Since the model random process is Guassian, it is completely determined by its mean and autocorrelation, and any of its moments can be found from them. In particular, the expression inside the above integral is given by

$$E\{n^2(t)n^2(s)\} = 2\sigma_n^4 \exp(-2b|t-2|) + \sigma_n^4 \tag{A12}$$

Integrating this expression, one finds

$$E\{[\int_0^T n^2(t)dt]^2\} = \frac{\sigma_n^4}{b^2}[2bT + \exp(-2bT) - 1] + T^2\sigma_n^4 \qquad \text{(A13)}$$

Also,

$$\begin{aligned} E\{[\frac{1}{T}\int_0^T n^2(t)dt]^2\} &= \frac{1}{T^2}E\{[\int_0^T n^2(t)dt]^2\} \\ &= \frac{\sigma_n^4}{b^2T^2}[2bT + \exp(-2bT) - 1] + \sigma_n^4 \qquad \text{(A14)} \end{aligned}$$

To get the variances, the squares of the means are subtracted from the above expressions:

$$\text{Var}\,[\int_0^T n^2(t)dt] = \frac{\sigma_n^4}{b^2}[2bT + \exp(-2bT) - 1] \qquad \text{(A15)}$$

$$\text{Var}\,[\frac{1}{T}\int_0^T n^2(t)dt] = \frac{\sigma_n^4}{b^2T^2}[2bT + \exp(-2bT) - 1] \qquad \text{(A16)}$$

The first variance increases without bound as T increases; the second decreases to zero in the limit as T goes to infinity.

The final noise term to be analyzed is $\int_0^T n_1(t)n_2(t)dt$. The functions $n_1(t)$ and $n_2(t)$ represent noise processes at two different points in space; they are taken to have identical distributions given by the Gauss-Markov

process. For the conditions of Buck and Greene's technique to be met, $n_1(t)$ and $n_2(t)$ should be independent, but this will depend on the distance between the observation points.

A result of the frozen turbulence approximation [Ref. 24] is the property that the autocorrelation of homegeneous turbulence fluctuations in time at one point has the same form as the correlation of tubulence fluctuations in space (at a given instant of time). Thus, one has

$$R_n(\bar{r}_1, \bar{r}_2) = \sigma_n^2 \exp(-a||\bar{r}_1 - \bar{r}_2||) = \sigma_n^2 \exp(-ad) \qquad \text{(A17)}$$

where $\bar{r}_1$ and $\bar{r}_2$ are points in space and d is the distance between them. It should be noted that the intrinsic wind turbulence will probably not be strictly homogeneous in many cases of interest; the above expression is only a rough approximation. Also, if a significant part of the nonacoustic noise signal is due to the two microphones' own wake turbulence rather than to intrinsic turbulence, the correlation between the noise processes will obviously be much smaller, since in this case they are generated separately at the two points in space. The above spatial correlation expression does have the expected relationship of decreasing correlation for increasing microphone separation, so it is accepted here as a sufficiently good approximation.

The mean of the term $\int_0^T n_1(t)n_2(t)dt$ is given by

$$E\{\int_0^T n_1(t)n_2(t)dt\} = \int_0^T E\{n_1(t)n_2(t)\}\,dt \tag{A18}$$

But $E\{n_1(t)n_2(t)\} = R_n(\bar{r}_1, \bar{r}_2) = \sigma_n^2 \exp(-ad)$, independent of time t:

$$\begin{aligned} E\{\int_0^T n_1(t)n_2(t)dt\} &= \int_0^T \sigma_n^2 \exp(-ad)dt \\ &= T\sigma_n^2 \exp(-ad) \end{aligned} \tag{A19}$$

and also

$$E\{\frac{1}{T}\int_0^T n_1(t)n_2(t)dt\} = \sigma_n^2 \exp(-ad) \tag{A20}$$

Thus, the means are close to zero if the observation points are far enough apart; the first does increase linearly with T, however. To find the variances, one first evaluates $E\left\{\left[\int_0^T n_1(t)n_2(t)dt\right]^2\right\}$:

$$\begin{aligned} E\{|\int_0^T n_1(t)n_2(t)dt|^2\} &= E\{\int_0^T n_1(t)n_2(t)dt \int_0^T n_1(s)n_2(s)ds\} \\ &= \int_0^T \int_0^T E\{n_1(t)n_2(t)n_1(s)n_2(2)\}dtds \end{aligned} \tag{A21}$$

To determine the expression inside the integral, one more piece of information is required: the correlation between the noise at one point and one

time ($n_1(t)$, for example) and the noise at another point and another time ($n_2(s)$). This can be modelled as

$$R_n(\bar{r}_1, t, \bar{r}_2, s) = \sigma_n^2 \exp(ad) \exp(-b\,|t-2|) \tag{A22}$$

based on the frozen turbulence approximation for homogeneous atmospheric turbulence [25]. Using this expression, the integrand is

$$\begin{aligned} E\{n_1(t)n_2(t)n_1(s)n_2(s)\} &= \sigma_n^4 \exp(-2ad) + \sigma_n^4 \exp(-2b\,|t-2|) \\ &+ \sigma_n^4 \exp(-2ad) \exp(-2b\,|t-s|) \end{aligned} \tag{A23}$$

where d is the distance between observation points 1 (n_1) and 2 (n_2). Integrating, one finds

$$\begin{aligned} E\{[\int_0^T n_1(t)n_2(t)dt]^2\} &= \frac{\sigma_n^4}{2b^2}[1+\exp(-2ad)][2bT+\exp(-2bT)-1] \\ &+ T^2\sigma_n^4 \exp(-2ad) \end{aligned} \tag{A24}$$

and also,

$$E\{[\frac{1}{T}\int_0^T n_1(t)n_2(t)dt]^2\} = \frac{1}{T^2}E\{[\int_0^T n_1(t)n_2(t)dt]^2\}$$

$$+ \quad \frac{\sigma_n^4}{2b^2T2}[1+\exp(-2ad)][2bT+\exp(-2bT)-1]$$

$$+ \quad \sigma_n^4 \exp(-2ad) \qquad \text{(A25)}$$

Subtracting the squares of the means, one has the variances:

$$\mathrm{Var}[\int_0^T n_1(t)n_2(t)dt] = \frac{\sigma_n^4}{2b^2}[1+\exp(-2ad)][2bT+\exp(-2bT)-1] \quad \text{(A26)}$$

and

$$\mathrm{Var}[\frac{1}{T}\int_0^T n_1(t)n_2(t)dt] = \frac{\sigma_n^4}{2b^2T^2}[1+\exp(-2ad)][2bT+\exp(-2bT)-1] \quad \text{(A27)}$$

As with the previous set of variances, the first of these increases linearly with (large) T, and the second decreases to zero as T goes to infinity. Suprisingly, the separation d of the observation points has only a small effect on the variances; but this is reasonable because the observation point separation should have only a limited effect on the magnitude of fluctuations between the noise processes at the two points. Note that as d goes to zero, the means and variances above reduce to those for the $\int_0^T n^2(t)dt$ noise term, as they should. Although the assumptions leading to the variance expressions are based in part on conjecture, the expressions themselves appear to be

reasonable descriptions of the dependence of the noise term characteristics on the measurement period T and the observation point spacing d.

USACERL Distribution

Chief of Engineers
ATTN: CEMP-CE
ATTN: CEMP-EA
ATTN: CEMP-EI (2)
ATTN: CEMP-ZA
ATTN: CEMP-ZM (2)
ATTN: CEHSC-IM-LP (2)
ATTN: CEHSC-IM-LH (2)
ATTN: CERD-L

Army Environmental Office 20310
ATTN: ENVR-EP

HQ USAF/LEEEU 20332

AMC 22333
ATTN: AMCEN-A

Naval Air Systems Command 20360
ATTN: Library

Little Rock AFB 72099
ATTN: 314/DEEE

Aberdeen PG, MD 21010
ATTN: Safety Office Range Safety Div
ATTN: US Army Ballistic Res Lab (2)
ATTN: ARNG Operating Activity Ctr
ATTN: Human Engineer Lab

Edgewood Arsenal, MD 21010
ATTN: HSHB-MO-B

Ft. Belvoir, VA 22060
ATTN: NACEC-FB
ATTN: CECC-R

NAVFAC 22332
ATTN: Code 2003

Naval Surface Weapons Center 22448
ATTN: N-43

Ft. McPherson, GA 30330
ATTN: AFEN-FEB

US Army Acromedical Res Lab 36362
ATTN: SGRD-UAS-AS

USAWES 39180
ATTN: WESSEN-B
ATTN: Soils & Pavements Lab
ATTN: C/Structures

Wright-Patterson AFB, OH 45433
ATTN: AAMRL/BB
ATTN: AAMRL/BBE

Ft. Monmouth 07703
ATTN: AMSEL-EW-MD

WASH DC 20410
ATTN: Housing & Urban Dev (2)

Nat'l Institute of Standards & Tech 20899
ATTN: Force & Acoustics Group

Department of Transportation
ATTN: Library 20590

Naval Undersea Center, Code 401 92132

Bureau of National Affairs 20037

Building Research Board 20418

Transportation Research Board 20418

Federal Aviation Administration 20591

Defense Technical Info. Center 22314
ATTN: DDA (2)

45
+35
05/90